HAL
open science

The GM-CSF released by airway epithelial cells orchestrates the mucosal adjuvant activity of flagellin

Aneesh Vijayan, Laurye van Maele, Delphine Fougeron, Delphine Cayet, Jean Claude Sirard

To cite this version:

Aneesh Vijayan, Laurye van Maele, Delphine Fougeron, Delphine Cayet, Jean Claude Sirard. The GM-CSF released by airway epithelial cells orchestrates the mucosal adjuvant activity of flagellin. Journal of Immunology, 2020, pp.ji2000746. inserm-02957765

HAL Id: inserm-02957765

https://inserm.hal.science/inserm-02957765v1

Submitted on 5 Oct 2020

HAL is a multi-disciplinary open access archive for the deposit and dissemination of scientific research documents, whether they are published or not. The documents may come from teaching and research institutions in France or abroad, or from public or private research centers.

L'archive ouverte pluridisciplinaire **HAL**, est destinée au dépôt et à la diffusion de documents scientifiques de niveau recherche, publiés ou non, émanant des établissements d'enseignement et de recherche français ou étrangers, des laboratoires publics ou privés.

The GM-CSF released by airway epithelial cells orchestrates the mucosal adjuvant activity of flagellin

Aneesh Vijayan[*,†], Laurye Van Maele[*], Delphine Fougeron[*], Delphine Cayet[*], and Jean-Claude Sirard[*,‡]

[1] Univ. Lille, CNRS, Inserm, CHU Lille, Institut Pasteur de Lille, U1019 – UMR9017 - CIIL - Center for Infection and Immunity of Lille, F-59000 Lille, France

† Current address: Janssen Vaccines and Prevention B.V, Netherlands

‡ Funding: The study was funded by INSERM, Institut Pasteur de Lille, and Université de Lille. This project has received funding from the European Union's Horizon 2020 research and innovation programme under the Marie Skłodowska-Curie grant agreement No. 657107 to AV.

Running title : Key role of epithelial GM-CSF for mucosal adjuvant

ABSTRACT

The Toll-like receptor 5 (TLR5) agonist flagellin is a potent adjuvant and is currently being developed for use in vaccines. The mechanisms that drive flagellin's activity are influenced by its administration route. Previous studies showed that lung structural cells (especially epithelial cells lining the conducting airways) are pivotal for the efficacy of intranasally administered flagellin-containing vaccines. Here, we looked at how the airway epithelial cells regulate the flagellin-dependent stimulation of antigen-specific $CD4^+$ T cells and the antibody response in mice. Our results demonstrate that after sensing flagellin, airway epithelial cells trigger the release of granulocyte-macrophage colony-stimulating factor (GM-CSF) in a TLR5-dependent fashion and the doubling of the number of activated type 2 conventional dendritic cells (cDC2s) in draining lymph nodes. Furthermore, the neutralization of GM-CSF reduced cDC2s activation. This resulted in lower of antigen-specific $CD4^+$ T cell count and antibody titers in mice. Our data indicate that during pulmonary immunization, the GM-CSF released by airway epithelial cells orchestrates the cross-talk between cDC2s and $CD4^+$ T cells and thus drives flagellin's adjuvant effect.

SINGLE-SENTENCE KEY POINTS

- Flagellin induces GM-CSF production by airway epithelial cells
- GM-CSF transactivates lung conventional dendritic cells
- GM-CSF drives the mucosal adjuvant activity of flagellin/TLR5 signaling

38 **INTRODUCTION**

39 Vaccines against infectious diseases is based on the administration of protective, immunodominant
40 antigens that trigger antibody and T cell responses and thus result in the neutralization or death of
41 the pathogenic microorganisms. Most antigens are formulated in a way that enables a rapid,
42 intense, and long-lasting protective response. To optimize immunization, adjuvants can be
43 included to vaccines in order to promote targeting and stimulation of the innate immune system –
44 both of which are essential for an appropriate vaccine response (1).

45 Toll-like receptor (TLR) agonists trigger innate immune responses and are used as adjuvant of
46 vaccination. There are many evidences that TLR signaling enhances vaccine efficacy by
47 effectively priming the adaptive immune system (2-5). In the context of vaccination, the cells that
48 respond primarily to TLR agonists include professional antigen-presenting cells (APCs) such as
49 dendritic cells (DCs), B lymphocytes or macrophages. However, many structural cells including
50 epithelial cells ubiquitously express pattern recognition receptors (PRRs) - including TLRs – and
51 therefore respond to TLR agonists (6-11) . There is a large body of literature data on how
52 monophosphoryl lipid A (an attenuated lipopolysaccharide derivative used in adjuvant
53 formulation) influences structural and myeloid cells at the site of vaccine injection (2, 12-14).
54 Indeed, monophosphoryl lipid A triggers TLR4 signaling in the structural cells, which in turn
55 contributes to the vaccine's efficacy.

56 Bacterial flagellin is a TLR5 agonist and acts as a potent systemic and mucosal adjuvant (15).
57 Although DCs are essential for flagellin's adjuvanticity, the process that drives DC activation is
58 strongly influenced by the immunization route. The adjuvant activity is driven either by the direct
59 or indirect activation of APCs (especially DCs) (16-22). For example, the long-term, T-cell-
60 dependent antibody response against systemically administered flagellin from *Salmonella* (FliC)

61 depends on TLR5 signaling in $CD11b^{+}CD103^{+}$ double-positive conventional DCs (cDCs) (21-23).
62 In contrast, the delivery of flagellin to the mucosae (especially the airways) potentiates first-line
63 adaptive responses by structural cells (especially airway epithelial cells, AECs) (24-28). Thus,
64 intranasal or intratracheal administration of flagellin induces immediate and transient TLR5
65 signaling in lungs (16, 25, 26, 29, 30). Notably, experiments bone-marrow chimera and
66 microdissection of lung tissue showed that flagellin activates the structural epithelial airway cells
67 but does not impact on the alveolar macrophages. TLR5-mediated activation of AECs, in turn
68 activates lung DCs (16, 27, 28, 31) However, the underlying mechanism remains poorly
69 understood. Airway epithelial cells respond to flagellin by releasing a broad range of cytokines
70 and chemokines (such as CCL20, IL-1α, or IL-1β) that may impact lung DC maturation. It has
71 been suggested that the AEC-derived cytokines IL-25, IL-33 and thymic stromal lymphopoietin
72 (TSLP) promote DC activation (27, 28). Furthermore, AEC stimulation by flagellin enhances the
73 influx of neutrophils and monocytes that may contribute as APCs. Recently, we showed that
74 neither the IL-1 cytokine family nor neutrophils nor monocytes orchestrate flagellin's mucosal
75 adjuvant activity (16). In experiments in the mouse (and in contrast to cholera toxin subunit B, a
76 potent mucosal adjuvant), intranasally administered recombinant flagellin did not enter into the
77 lung parenchyma and thus could not activate the DCs located there (16, 26). We therefore sought
78 to establish how cross-talk between AECs and lung cDCs promotes flagellin's mucosal adjuvant
79 effect. To this end, we used an *in vitro* model based on (i) murine AECs grown at the air-liquid
80 interface (ALI), and (ii) FMS-like tyrosine kinase 3 Ligand (FLT3L)-derived cDCs from murine
81 bone marrow. We demonstrated that flagellin-stimulated AECs release GM-CSF in a TLR5-
82 dependent manner and thus enhance the frequency of activated type 2 $CD11b^{+}$ DCs (cDC2s).
83 Furthermore, activated cDCs loaded with an MHCII-restricted ovalbumin (OVA) peptide primed

84 OVA-specific $CD4^+$ T cell (OTII cells) and prompted rapid proliferation of the latter. Disruption
85 of GM-CSF signaling abrogated the flagellin- and AEC-dependent activation of cDCs and the
86 subsequent activation of OTII cells. We next tested the effect of flagellin-induced GM-CSF on
87 lung cDCs *in vivo*. Epithelium-derived GM-CSF significantly increased the frequency of cDC2s
88 in the lung-draining mediastinal lymph nodes (MdLNs). In mice, the antibody-based blockade of
89 GM-CSF signaling reduced the number of activated cDC2 in the MdLNs. In turn, this drastically
90 reduced titers of antigen-specific $CD4^+$ T-cell-dependent IgG antibodies. Taken as a whole, our
91 results suggest that AEC-derived GM-CSF initiates the cross-talk between lung $CD11b^+$ cDCs and
92 antigen-specific T cells, and thus promotes the mucosal adjuvant effect of flagellin.
93

94 **MATERIALS AND METHODS**

95 **Ethics statement.** Animals were maintained in a pathogen-free facility in compliance with
96 institutional guidelines at the Institut Pasteur de Lille (animal facility agreement #C59-350009).
97 All experiments complied with current national, institutional and European regulations and ethical
98 guidelines, were approved by our Institutional Animal Care and Use Committee (reference:
99 APAFIS#5164, protocol 2015121722429127_v4) and were conducted by qualified, accredited
100 personnel.

101 **Animals**

102 Six- to eight-week-old female C57BL/6JRj mice (Janvier Labs, Saint Berthevin, France), OT-II,
103 *Tlr4*$^{-/-}$ and *Tlr5*$^{-/-}$ mice (backcrossed on C57BL/6J) were used.

104 **Reagents**

105 The custom-designed flagellin primarily used in the present study (recombinant flagellin FliC$_{\Delta 174-}$
106 $_{400}$ harboring a carboxy-terminal histidine Tag) derives from *Salmonella enterica* serovar
107 Typhimurium FliC (32, 33). The recombinant FliC$_{\Delta 174-400/89-96*}$ (referred to henceforth as
108 FliC$_{TLR5mut}$, and which does not signal through TLR5) was generated by replacing the residues
109 involved in TLR5 detection (89-96, QRVRELAV) with the corresponding sequence from a non-
110 signaling flagellin (DTVKVKAT) (29, 32, 33). The recombinant flagellins were expressed in
111 inclusion bodies in *Escherichia coli* BL21(DE3) and then purified to homogeneity with metal
112 affinity, ion-exchange, gel filtration and fast protein liquid chromatography techniques (GE
113 Healthcare, Pittsburgh, PA) after endotoxin depletion. Using a *Limulus* assay (Pierce LAL
114 Chromogenic Endotoxin Quantitation Kit, Thermo Fisher Scientific, Waltham, MA), we estimated
115 the final endotoxin content in the protein preparation to be 0.016 endotoxin units per µg of protein.
116 The molecular consistency and biological activity of FliC$_{\Delta 174-400}$ and FliC$_{TLR5mut}$ were quality-

117 controlled as described in **Supplementary Figure 1 A-C**. Endograde OVA (Hyglos, Bernried,
118 Germany) and OVA-specific MHCII-restricted peptide (Invivogen, San Diego, CA) were used in
119 the present study. The anti-GM-CSF antibody (clone MP1-2EE9) and the isotype control (clone
120 2A3) were obtained from BioXcell, West Lebanon, NH. Recombinant murine FMS-like tyrosine
121 kinase 3 ligand (FLT3L) was purchased from Peprotech, Neuilly-Sur-Seine, France.

122 **Immunization and sample collection**

123 Mice were lightly anesthetized (using gaseous isoflurane) prior to intranasal
124 immunization/treatment in a maximum volume of 30 μl. Unless otherwise specified, a homologous
125 prime-boost immunization protocol was used to assess the specific adaptive immune responses to
126 OVA (10 μg) as the model antigen and the flagellin $FliC_{\Delta 174\text{-}400}$ (2 μg) as the adjuvant. For cDC
127 activation and time-course studies, mice were sacrificed at 6 hours and 18 hours following
128 intranasal instillation of FliC (2 μg). For GM-CSF depletion studies, animals were treated with
129 60 μg of GM-CSF-specific antibody or isotype control 2 hours prior to immunization, with an
130 additional 60 μg of antibody then administered intranasally at the same time as the flagellin and/or
131 OVA. Bronchoalveolar lavage (BAL), MdLNs, lung, spleen and serum samples were collected as
132 described previously (16, 26, 32). Lung extract were prepared by homogenizing the lung in 2 ml
133 of Tissue Protein Extraction Reagent (Pierce, Rockford, IL).

134 **Antigen-specific immune responses.**

135 Titers of OVA-specific antibodies in serum and BAL samples were assessed using an ELISA. The
136 ELISA plates were prepared by absorption of OVA (1 μg/ml in phosphate-buffered saline (PBS))
137 or anti-mouse IgG (5 μg/ml in PBS; product 1031-01 from SouthernBiotech, Birmingham, AL)
138 overnight at 4 °C on Maxisorp microplates (Nunc, Rochester, NY), and blocking for 1 h at room
139 temperature with 1% dried milk in PBS. Next, the ELISA plates were incubated for 1 h at room

140 temperature with serial dilutions (for coated plates) of the serum samples or (for anti-mouse IgG-
141 coated plates) of IgG standards (IgG, I5381, Sigma-Aldrich, Saint Louis, MO). Primary antibody
142 binding was revealed by subsequent incubations with a biotin-conjugated goat anti-mouse IgG
143 antibody (SouthernBiotech), a peroxidase-streptavidin complex (RPN1231, GE Healthcare,
144 Chicago, IL), and tetramethylbenzidine (555214, BD Biosciences, Franklin lakes, NJ), and
145 measured using a microplate reader at wavelengths of 450 and 570 nm. Absolute quantities of
146 antibodies were calculated according to standard curves and expressed in ng/ml.

147 **Cytokine production.** Cytokine levels in serum, BAL, lung extract or cell culture supernatants
148 were measured using commercial ELISA kits for GM-CSF, IL-2, CCL20 (all from R&D Systems,
149 Minneapolis, MN) and IFNγ (Invitrogen, Carlsbad, CA).

150 **Air-liquid interface (ALI) cultures of AECs, and the production of conditioned medium**

151 Mouse AEC cultures were established as described previously (34, 35). The AECs were isolated
152 by overnight incubation of mouse trachea with 0.15% pronase (Roche) at 4ºC. The cells were
153 seeded on collagen-coated Transwell® inserts (Corning™, Corning, NY; one insert per mouse).
154 The ALI cultures were established once the cells' transepithelial resistance exceeded 1000 Ωcm^2
155 (usually within one week). The medium was then removed from the apical side. The AECs were
156 treated by adding 10 µl of 1 µg/ml of flagellin $FliC_{\Delta 174-400}$ or PBS alone (control) to the apical side
157 of the insert. The conditioned medium was collected from the basal compartment after 24 h,
158 aliquoted, and stored at -80ºC prior to the cytokine assay or to treatment of DCs.

159 **Production of FLT3L-derived bone marrow DCs**

160 Conventional DCs were derived from the bone marrow (BM) of animals, as described previously
161 (36, 37). Briefly, BM cells were isolated from mice, and any red blood cells were lysed. Next, 10^7
162 cells were suspended in 5 ml of RPMI complete medium supplemented with 100 ng/ml of mouse

163 recombinant FLT3L (Peprotech). The cells were seeded into a single well of a 6-well plate (Ultra-
164 low binding, Corning™). After 3 days of culture, the cell suspension was divided into two
165 volumes, and 2.5 ml of fresh medium supplemented with 100 ng/ml of recombinant FLT3L was
166 added to each. The process was repeated on day 6, and the cells were ready to use on day 9.

167 **Flow cytometry**

168 Cell suspensions of lung, MdLNs or spleen were obtained by enzymatic digestion with collagenase
169 from *Clostridium* type IA (1 mg/mL, Sigma-Aldrich) and DNAse I (40 µg/ml, Sigma-Aldrich) for
170 30 min at 37°C. For lungs, hematopoietic cells were recovered after centrifugation on Percoll 20%
171 (GE Healthcare), incubated with anti-CD16/CD32 FcR blocking antibodies (clone 2.4G2), and
172 then stained with specific antibodies. The following antibodies were used to study tissue cells and
173 BMDC populations: anti-Gr1-FITC (clone RB6-8C5, BioLegend, San Diego, CA), anti-CD3ε-
174 FITC (clone 145-2C11, BD Biosciences), anti-B220-FITC (clone RA3-6B2; BioLegend), anti-
175 CD64-PE (clone X54-5/7.1; BioLegend), anti-SiglecF-AF647 (clone E50-2440; BD Biosciences),
176 anti-CD11b-BV786 (clone M1/70; BioLegend), anti-MHC II-PB (clone M5/114.15.2;
177 BioLegend), anti-CD11c-PE/Cy7 (clone N418; BioLegend), anti-CD24-PerCP-Cy5.5 (clone
178 M1/69; BioLegend), anti-CD45-APC-Cy7 (clone 30F11; BioLegend), anti-CD86-BV605 (clone
179 GL1; BioLegend), anti-CD80-PE/Cy5 (clone 16-10A1; BioLegend). To study vaccine-induced
180 OVA-specific T cells: anti-CD3ε -FITC, anti-CD4-APC/Fire750 (clone RM4-5; BioLegend), anti-
181 CD8-PeCy7 (clone 53-6.7; BioLegend), anti-CD45-BV650 (clone 30F11; BioLegend) and
182 CellTrace™ Violet (CTV; Invitrogen) were used. Dead cells were excluded from the analysis by
183 using Live/Dead Aqua dye (Invitrogen). Cells were stained with surface-specific antibodies for
184 30 min at 4ºC. Data were collected on a BD LSR Fortessa (BD Biosciences) and analyzed with
185 FlowJo software (V10).

186 **Gene expression analysis**

187 Total RNA from AECs was isolated with a Nucleospin RNA kit (Macherey-Nagel). The RNA was
188 reverse-transcribed with a High-Capacity cDNA Archive Kit (Applied Biosystems), according to
189 manufacturer's instructions. Gene expression was quantified by cDNA amplification in a
190 QuantStudio 12K real-time PCR system (Applied Biosystems, Foster City, CA), using Power
191 SYBR® Green PCR Master Mix (Applied Biosystems). Relative mRNA levels (2-ΔΔCt) were
192 determined by comparing (i) the cycle thresholds (Ct) for the gene of interest and for *Actb* (ΔCt)
193 and (ii) the ΔCt values for treated and control groups (ΔΔCt). The upper boundary for Ct was set
194 to 35 cycles.

195 **Co-cultures of CD4 lymphocytes and DCs.**

196 CD4 cells were isolated from the lymph nodes and spleen of OTII mice, using negative selection
197 (CD4 isolation kit, Miltenyi Biotec, Bergisch Gladbach, Germany). The cells were next stained
198 with CTV, according to manufacturer's instructions. The conditioned media from flagellin- or
199 PBS-treated AECs were incubated with 10 µg/ml of anti-GM-CSF or isotype antibody for
200 30 minutes at 37°C. FLT3L-derived BMDCs were treated with the antibody-pre-incubated, AEC-
201 conditioned media for 18 hours. After washing with RPMI medium, the DCs were loaded with
202 2 µg/ml of MHCII-restricted, OVA-specific peptide ($OVA_{323-339}$; Invivogen). Following a 4-hour
203 incubation at 37ºC, the DCs were washed and then incubated with CTV-stained CD4 T cells at a
204 ratio of 1:20 for 4 days. The proliferation of OT-II cells was assessed using flow cytometry.

205 **Statistics**

206 Statistical analysis was performed using GraphPad Prism version 8 software (San Diego, CA).
207 Groups were compared using a Mann-Whitney test (for two independent groups) or Kruskal-

208 Wallis one-way ANOVA with Dunn's post-test (for three or more groups). Unless otherwise
209 specified, the results were expressed as the mean ± standard error of the mean (SEM).
210

211

212 **RESULTS**

213 ***Flagellin's activity as a mucosal adjuvant is dependent on TLR5 signaling and CD4$^+$T cells***

214 To confirm the involvement of TLR5 signaling in flagellin's mucosal adjuvant activity, mice were
215 immunized intranasally on days 0 and 21 with ovalbumin alone or formulated with FliC$_{\Delta 174\text{-}400}$ or
216 FliC$_{TLR5mut}$ (i.e. the counterpart with a defect in TLR5 signaling). We found that mice immunized
217 with OVA and FliC$_{TLR5mut}$ had very low serum OVA-specific antibody titers similar to mice
218 immunized with OVA only (**Figure 1A**). In contrast, a combined formulation of OVA and
219 FliC$_{\Delta 174\text{-}400}$ was associated with 100-fold more elevated titers of serum OVA-specific antibodies.
220 The specific *ex vivo* stimulation of lung-draining MdLN cells with OVA enhanced CD4$^+$ T cell but
221 not CD8$^+$ T proliferation solely in animals that had received FliC$_{\Delta 174\text{-}400}$ and OVA (**Figure 1B**).
222 Concordantly, OVA-stimulated MdLN cells secreted high levels of IFNγ and IL-2 when animals
223 were immunized with FliC$_{\Delta 174\text{-}400}$ (**Supplementary Figure 1D**). However, this effect of
224 immunization was not observed with cells isolated from spleen or lungs since no cytokines were
225 detectable in supernatant of OVA-stimulated cells. Since the elevation in the antigen-specific
226 CD4$^+$ T cell count was correlated with the serum antibody titer, we further evaluated the
227 contribution of CD4$^+$ T cells to flagellin's mucosal adjuvant activity. Antibody-based depletion of
228 CD4$^+$ T lymphocytes prior to immunization drastically reduced the levels of OVA-specific
229 antibodies (**Figure 1C**). Taken as a whole, these results demonstrated that FliC$_{\Delta 174\text{-}400}$'s mucosal
230 adjuvant activity is TLR5-dependent and requires antigen-specific CD4$^+$ T cells.

231

232 ***Airway epithelial cells sense flagellin via TLR5 to release GM-CSF***

233 We and others have found that AECs are the primary targets for flagellin's mucosal activity (24-
234 28). The AECs that make up a large proportion of lung structural cells release chemokines and
235 cytokines, which in turn can recruit DCs, modulate the cells' functions, and shape a potent immune
236 response. We therefore sought to investigate the DC-modulating cytokines that are released by
237 AECs in response to flagellin. To this end, we studied cultures of tracheal epithelial cells from *in*
238 *vitro* ALI cultures. The cells differentiated into a complex set of AECs that recapitulated the cell
239 composition and structures found in the bronchial epithelium. We found that administration of
240 flagellin $FliC_{\Delta 174\text{-}400}$ at the air interface stimulated the expression of several genes linked to innate
241 immune signaling (**Figure 2A**). We observed that the mRNA expression of the *Csf2*gene (coding
242 for GM-CSF) was significantly upregulated (~10 fold) 2 hours after flagellin treatment, whereas
243 the genes for other DC-modulating cytokines (such as TSLP, IL-33 and IL-25) were not affected.
244 Moreover, the polarized secretion of GM-CSF into the basal compartment of flagellin-stimulated
245 AECs was enhanced after 24 hours (**Figure 2B**). Next, we probed the contribution of TLR5
246 signaling on AECs to the production of GM-CSF, using AECs from *Tlr5*$^{-/-}$ mice. We found that
247 *Tlr5*$^{-/-}$ AECs did not secrete any GM-CSF when stimulated with $FliC_{\Delta 174\text{-}400}$ (**Figure 2C**).
248 Similarly, we demonstrated that freshly isolated alveolar epithelial cells
249 ($CD45^{neg}CD31^{neg}Ter119^{neg}Epcam^{+}$) from naïve animals were stimulated by flagellin to upregulate
250 *Csf2* mRNA levels, whereas this did not occur in cells from *Tlr5*$^{-/-}$ animals
251 (**Supplementary Figure 2A-B**). Using intranasal flagellin instillation, we next investigated
252 whether GM-CSF could be detected in the respiratory compartments. In agreement with our *in*
253 *vitro* observations, GM-CSF was detected in the BAL (**Figure 2D**) of animals - most prominently
254 4 hours after the treatment. Interestingly, GM-CSF production was upregulated in mouse BAL
255 after the administration of the native form flagellin FliC, whereas TSLP, IL-33 and IL-25 were

256 barely detected (**Supplementary Figure 2C-D**). These data suggest that AECs detect flagellin and
257 promote the secretion of GM-CSF in a TLR5-dependent manner.
258
259 ***Type 2 cDCs respond to GM-CSF released by flagellin-stimulated AECs***
260 Since lung-resident cDC2 are required for flagellin's adjuvant effect, we next looked at how AECs
261 interact with cDC2. To this end, total mouse BM cells were differentiated into cDCs using the
262 growth factor FLT3L. The resulting cells closely resembled the DC population found in murine
263 tissues, including cDC1s, cDC2s, and plasmacytoid DCs. To circumvent any direct activation of
264 DCs by flagellin, we generated FLT3L-derived cDCs from *Tlr5*$^{-/-}$ mice. The conditioned medium
265 collected from the basal compartment of the flagellin FliC$_{\Delta 174\text{-}400}$-treated AECs was incubated with
266 FLT3L-derived cDCs and compared with mock-conditioned AEC medium (**Figure 3A**). Our
267 initial experiments demonstrated that flagellin-conditioned medium was able to influence DCs.
268 This stimulation was characterized by an enhanced number of activated cDC2s, as demonstrated
269 by the increased frequency of the CD80^{+}CD86^{+}-expressing CD11b^{+}CD24^{dim} cDC2 population.
270 Since GM-CSF production was identified as being differentially regulated by FliC$_{\Delta 174\text{-}400}$, we
271 addressed the factor's contribution to DC maturation by neutralizing it with a specific monoclonal
272 antibody (**Figure 3B-C**). The neutralization of GM-CSF in flagellin-conditioned medium was
273 associated with a significantly lower mean ± SD frequency of activated cDC2s (46.5±4.95%),
274 relative to the control group of isotype-treated cells (72.4±6.26%). Moreover, the expression of
275 the activation markers CD80 and CD86 was significantly higher when for cells exposed to
276 flagellin-conditioned AEC medium and the isotype antibody, compared with mock-conditioned
277 controls. This effect was completely blocked by GM-CSF-specific antibodies (**Figure 3C**). Taken

278 as a whole, these data demonstrated that the GM-CSF produced by flagellin-stimulated AECs is
279 essential for regulating the number and activation status of FLT3L-derived cDC2s.
280
281 ***GM-CSF improves the ability of cDCs to prime antigen-specific CD4$^+$ T cells***
282 To determine the contribution of GM-CSF-exposed cDC to the priming of CD4$^+$ T cells, we carried
283 out an *in vitro* experiment with conditioned-medium-treated, OVA-specific MHCII peptide-
284 loaded-DCs and CD4$^+$ T lymphocytes from OTII mice (**Figure 4A**). Briefly, FLT3L-derived DCs
285 that had been exposed to AEC-conditioned medium and antibodies were loaded with MHCII-
286 restricted OVA$_{323-339}$ peptide prior to incubation with CTV-labeled OVA-specific CD4$^+$ T cells
287 from OT-II mice. By measuring the dilution of CTV, we evaluated the proportion of CD4$^+$ T cells
288 that had divided after exposure to antigen and DCs (**Figure 4B**). Mock-conditioned medium
289 promoted the division of about 18.9% of the CD4$^+$ T cells, whereas flagellin-conditioned medium
290 significantly promoted the division of proliferating CD4$^+$ T cells (25%) (**Figure 4B-C**). The
291 neutralization of GM-CSF during the incubation of DCs with flagellin-conditioned medium
292 strongly impaired T cell proliferation (**Figure 4C**). Remarkably, antibody treatment yielded
293 proliferation levels similar to those obtained with mock-conditioned medium.
294 Given the influence of the DC-T cell interaction on T cell priming, we sorted cDC2s from the
295 MdLN of mice that had been immunized with flagellin and OVA in the presence of a GM-CSF-
296 specific antibody prior to incubation with CTV-stained OTII cells (**Supplementary Figure 3A-**
297 **C**). Strikingly, cDC2s from anti-GM-CSF-treated mice were less efficient in priming the CD4$^+$ T
298 cells than cDC2s from mock mice. Therefore, our data suggest that the secretion of GM-CSF by
299 flagellin-stimulated AECs orchestrates CD4$^+$ T cell activation by promoting the functional
300 maturation of cDC2s.

301

302 ***Flagellin-dependent GM-CSF production in the lung enhances the number of cDC2s in MdLNs***

303 After being activated, lung cDCs migrate to the MdLNs, where they prime T cells and help to
304 mount an effective adaptive response (16, 26, 31). To validate our *in vitro* observations, we
305 determined whether or not flagellin-mediated GM-CSF production in the lung drive the increase
306 in the frequencies and activation status of MdLN DCs (**Figure 5A**). Using fluorescently labelled
307 OVA (OVA_{AF647}), we found that cDC2s are the predominant OVA-carrying DCs in the MdLNs
308 when this protein is given intranasally at the same time as flagellin (**Supplementary Figure 3D**).
309 Intranasal instillation of flagellin increased the cDC2s (as a proportion of total DCs), compared
310 with naïve animals (62% vs. 46%). In contrast, the proportion of cDC1s did not change
311 (**Figure 5B**). Concomitantly, we observed a significantly lower proportion (51%) of cDC2s in
312 animals that had received anti-GM-CSF antibody along with flagellin, relative to isotype-treated
313 animals) (**Figure 5C**). Furthermore, one third of the animals that received anti-GM-CSF antibody
314 had almost the same cDC2 levels as in naïve mice. Furthermore, the frequency of
315 $CD80^{+}CD86^{+}$ cDC2 was significantly lower in experiments with neutralized GM-CSF
316 (**Figure 5D**). Lastly, the cDC2s were less activated, as evidenced by the significantly lower median
317 fluorescence intensity for CD80 following GM-CSF-specific antibody treatment but not following
318 treatment with an isotype control (**Figure 5E**). Taken as a whole, these data show that flagellin-
319 driven GM-CSF production in the lung significantly upregulates the proportion of activated cDC2s
320 in lung-draining MdLNs.

321

322 ***In vivo neutralization of GM-CSF abrogates the mucosal adjuvant activity of flagellin***

323 To demonstrate that modulating the function and number of cDCs in the MdLN can affect
324 flagellin's mucosal adjuvant activity, we performed prime-boost immunization with flagellin and
325 OVA antigen at the same time as the treatment with an anti-GM-CSF antibody or an isotype control
326 (**Figure 6A**). After ex vivo stimulation with OVA, 1.53% of the MdLN CD4+ T cells isolated
327 from animals immunized with flagellin and OVA and then treated with an isotype antibody were
328 found to be dividing (**Figure 6B**). In contrast, the proportion of dividing $CD4^+$ T cells in animals
329 that received anti-GM-CSF was only 0.44%; this corresponded to a 3-fold relative reduction. To
330 check whether the number of antigen-specific $CD4^+$ T cells was correlated with the titer of antigen-
331 specific antibodies, OVA-specific antibodies were assayed in the serum and BAL of immunized
332 animals. Both titers were significantly lower in mice that received anti-GM-CSF antibody than
333 isotype-treated mice (**Figure 6C**). Furthermore, we did not observe any correlation between the
334 frequency of cDC1s and the titer of OVA-specific antibodies following GM-CSF neutralization
335 (R^2=0.21, p=0.0852) (**Supplementary Figure 3E**). However, we observed a strong, positive
336 correlation between the frequency of cDC2s and the titer of OVA antibodies (R^2=0.72, p<0.0001).
337 This correlation suggested that flagellin-dependent GM-CSF production in the lung is important
338 for mediating flagellin's adjuvant activity via cDC2 activation.
339

340 **DISCUSSION**

341 Airway epithelial cells are known to secrete factors that can influence a wide range of immune
342 cells in the lung (6). The AECs' ability to drive immunological changes during allergen exposure
343 has been well characterized. Our present data reveal a new role for AECs: promoting the mucosal
344 adjuvant activity of flagellin by the local production of GM-CSF and transactivation of lung DCs.
345 Our *in vitro* ALI cultures of AECs and DCs provided a comprehensive view of how GM-CSF
346 released from flagellin-stimulated AECs orchestrates the cross-talk between cDC2s and antigen-
347 specific $CD4^+$ T cells. This is consistent with *in vivo* data suggesting that GM-CSF recruits cDC2s
348 into lung-draining lymph nodes and thus helps to prime antigen-specific $CD4^+$ T cells. These
349 results underline the importance of GM-CSF production by AECs in flagellin's adjuvant activity.
350 GM-CSF is a pleiotropic cytokine expressed by both hematopoietic and non-hematopoietic cells,
351 and is known to regulate the proliferation and differentiation of various hematopoietic cells,
352 including DCs (38). The release of GM-CSF by AECs and the critical role of the GM-CSF receptor
353 in the development of DCs in nonlymphoid tissue suggest the existence of cross-talk between
354 structural cells and hematopoietic cells (39-43). The expression of *Csf2* in flagellin-stimulated
355 alveolar epithelial cells and in ALI AEC cultures was upregulated (**Figure 2 and Supplementary**
356 **Figure 2**). This finding was further corroborated by the low levels of GM-CSF expression in
357 flagellin-treated *Tlr5*$^{-/-}$ AECs, and also fits with our previous report in which the flagellin-driven
358 expression of *Csf2* in murine lungs was restricted to radioresistant structural cells (26). These
359 results are in agreement with observations in which nasal epithelial cells upregulate the production
360 of GM-CSF (43). Further investigations using conditional knockout models where the *Tlr5* and
361 *Csf2* genes are inactivated in the airway epithelial cell compartments will be instrumental to

362 demonstrate unambiguously that the flagellin-mediated adjuvant activity is dependent on GM-CSF
363 released by AECs.
364 Recent research has suggested that DC influence flagellin's mucosal activity when the adjuvant is
365 delivered at the surface of airway mucosa lining either nasal or lung tissue (16, 27, 31, 43). The
366 functional activation of DC is not due to direct TLR5 signaling in DC (such as transepithelial DC)
367 but rather to activation relayed by TLR5-stimulated epithelium. Our study demonstrated that the
368 adjuvant effect is primarily driven by cDC2s. It remains to be determined how GM-CSF
369 specifically impacts cDC2. The cDC2 phenotype can vary from the $CD11b^{+}$ profile found in the
370 lungs to the $CD103^{+}CD11b^{+}$ profile found in the gut's mucosal compartment. By using FLT3L-
371 derived BMDCs that are known to give rise to cDC2s and cDC1s (i.e. cells that closely resemble
372 the cDCs found in the lung), we were able to identify the role of the cDC2s. Since flagellin can
373 directly activate cDC2s (21-23) (due to their TLR5 expression), we used cDCs from *Tlr5*$^{-/-}$ animals
374 in order to analyze solely the flagellin-independent activation effect. It appears that native flagellin
375 (and probably the recombinant flagellin $FliC_{\Delta 174\text{-}400}$ used in the present study) is rapidly degraded
376 in the airways and translocates poorly in the lung parenchyma (26). Hence, the activation of cDC2s
377 by flagellin in the lung mucosal compartment is dependent on factors that are released by AECs.
378 We demonstrated here that GM-CSF released by $FliC_{\Delta 174\text{-}400}$-stimulated AECs can activate cDC2s
379 both *in vitro* and *in vivo*. Our *in vitro* data on FLT3L-derived cDCs stimulated with conditioned
380 medium from $FliC_{\Delta 174\text{-}400}$- activated AECs in the presence of GM-CSF-neutralizing antibodies
381 suggest that GM-CSF is a critical or at least important cytokine in the process of cDC2 maturation
382 (**Figure 3**). Next, GM-CSF neutralization studies in flagellin-treated mice concurred with the *in*
383 *vitro* observations and evidenced a significantly lower number of activated cDC2s in the lung-
384 draining lymph nodes (**Figure 4**). This finding is in line with literature reports on the importance

385 of GM-CSF as a key mediator of DC-driven responses to aero-allergens (41, 44, 45) but contrasts
386 with previous reports in which flagellin-activated AECs promoted adaptive immunity through
387 TSLP, IL-25 or IL-33 (27, 28). This difference may be due to the various flagellins that were used,
388 especially the native form that harbors the hypervariable domain, and display a stronger TLR5-
389 stimulating activity than the recombinant flagellin $FliC_{\Delta 174\text{-}400}$ (32). Consistently, a recent study
390 highlighted that the hypervariable domain of flagellin contributes to the magnitude of TLR5
391 signaling (46).
392 The current paradigm suggests that cDC2s in lung-draining lymph nodes are ideally placed to
393 prime $CD4^+$ T cells, whereas cDC1s mainly cross-present antigens to $CD8^+$ T cells (47). We found
394 a strong correlation between the number of cDC2s activated by AEC-derived GM-CSF on one
395 hand and frequency of antigen-specific $CD4^+$ T cells on the other. Co-culture experiments with
396 $CD4^+$ T cells and FLT3L-derived cDCs that had been exposed to the supernatant from flagellin-
397 stimulated AEC conditioned medium clearly showed the role of GM-CSF-licensed cDCs in
398 driving $CD4^+$ T cell proliferation (**Figure 5**). Moreover, the diminished antigen-specific $CD4^+$ T
399 cell response in flagellin-adjuvanted animals treated with GM-CSF antibodies clearly
400 demonstrated the importance of cDCs in $CD4^+$ T cell priming (**Figure 6**). These data correlate
401 with observations on flagellin impact on B cell response and IgA production at the nasal mucosa
402 (43).
403 The primary efficacy readout for many vaccines is the elicitation of antigen-specific antibodies,
404 which is usually dependent on $CD4^+$ T cells. Our data suggest that intranasal administration of
405 $FliC_{\Delta 174\text{-}400}$ efficiently primes antigen-specific $CD4^+$ T cells and elicits a strong mucosal and
406 systemic antibody response (**Figure 1**). In response to flagellin-adjuvanted intranasal
407 administration of OVA, a weak antigen-specific antibody response was observed in CD4-depleted

408 animals and in animals treated with GM-CSF-neutralizing antibodies (**Figure 6**). One possible
409 explanation for this would be a cascade effect of GM-CSF neutralization on cDC2s, which in turn
410 downregulates antigen-specific $CD4^+$ T cells and affecting overall antibody titers. It was recently
411 reported that cDC2s are efficient vectors in the T follicular helper-dependent antibody response,
412 due to their propensity to locate to the T-B cell border (48). Further work is needed to determine
413 whether GM-CSF has a role in the precise anatomic localization of cDC2s within lymph nodes.
414 Overall, our data suggest that GM-CSF has a critical role in triggering lung cDC2s to drive
415 flagellin's activity as a mucosal adjuvant. Determining how AECs and the GM-CSF they produce
416 affect cDC lung function and activation will constitute an important step in the development of
417 new respiratory adjuvants for vaccines against major pathogens.
418

419 **ACKNOWLEDGMENTS**

420 We thank Laurence Mulard and Sylvie Bay at Institut Pasteur, Paris for the mass spectometry
421 analysis.

422

423 **AUTHOR CONTRIBUTIONS**

424 AV performed all animal, RT-qPCR, ELISA, and flow cytometry experiments. DC prepared the
425 DC cultures and performed the experiments on the human airway epithelial cells. DF and LVM
426 performed the experiments with the native flagellin FliC. AV and JCS designed experiments and
427 wrote the manuscript. JCS supervised the experimental work as a whole.

428

429 **CONFLICT OF INTEREST**

430 The authors declare that the research was conducted in the absence of any commercial or financial
431 relationships that could be construed as a potential conflict of interest.

432

433 **DATA AND MATERIALS AVAILABILITY**

434 The raw data supporting the conclusions of this manuscript will be made available by the authors,
435 without undue reservation, to any qualified researcher.

436

437 **REFERENCES**

438 1. Del Giudice, G., R. Rappuoli, and A. M. Didierlaurent. 2018. Correlates of adjuvanticity:
439 A review on adjuvants in licensed vaccines. *Seminars in Immunology* 39: 14-21.
440 2. Mata-Haro, V., C. Cekic, M. Martin, P. M. Chilton, C. R. Casella, and T. C. Mitchell. 2007.
441 The vaccine adjuvant monophosphoryl lipid A as a TRIF-biased agonist of TLR4. *Science*
442 316: 1628-1632.
443 3. Pulendran, B. 2015. The varieties of immunological experience: of pathogens, stress, and
444 dendritic cells. *Annu Rev Immunol* 33: 563-606.
445 4. Wille-Reece, U., B. J. Flynn, K. Lore, R. A. Koup, A. P. Miles, A. Saul, R. M. Kedl, J. J.
446 Mattapallil, W. R. Weiss, M. Roederer, and R. A. Seder. 2006. Toll-like receptor agonists
447 influence the magnitude and quality of memory T cell responses after prime-boost
448 immunization in nonhuman primates. *J Exp Med* 203: 1249-1258.
449 5. Liang, F., G. Lindgren, K. J. Sandgren, E. A. Thompson, J. R. Francica, A. Seubert, E. De
450 Gregorio, S. Barnett, D. T. O'Hagan, N. J. Sullivan, R. A. Koup, R. A. Seder, and K. Lore.
451 2017. Vaccine priming is restricted to draining lymph nodes and controlled by adjuvant-
452 mediated antigen uptake. *Sci Transl Med* 9.
453 6. Whitsett, J. A., and T. Alenghat. 2015. Respiratory epithelial cells orchestrate pulmonary
454 innate immunity. *Nat Immunol* 16: 27-35.
455 7. Tan, A. M., H. C. Chen, P. Pochard, S. C. Eisenbarth, C. A. Herrick, and H. K. Bottomly.
456 2010. TLR4 signaling in stromal cells is critical for the initiation of allergic Th2 responses
457 to inhaled antigen. *J Immunol* 184: 3535-3544.
458 8. Zhang, Z., J. P. Louboutin, D. J. Weiner, J. B. Goldberg, and J. M. Wilson. 2005. Human
459 airway epithelial cells sense *Pseudomonas aeruginosa* infection via recognition of flagellin
460 by Toll-like receptor 5. *Infect Immun* 73: 7151-7160.
461 9. Hammad, H., M. Chieppa, F. Perros, M. A. Willart, R. N. Germain, and B. N. Lambrecht.
462 2009. House dust mite allergen induces asthma via Toll-like receptor 4 triggering of airway
463 structural cells. *Nat Med* 15: 410-416.
464 10. Sato, A., and A. Iwasaki. 2004. Induction of antiviral immunity requires Toll-like receptor
465 signaling in both stromal and dendritic cell compartments. *Proc Natl Acad Sci U S A* 101:
466 16274-16279.
467 11. Price, A. E., K. Shamardani, K. A. Lugo, J. Deguine, A. W. Roberts, B. L. Lee, and G. M.
468 Barton. 2018. A Map of Toll-like Receptor Expression in the Intestinal Epithelium Reveals
469 Distinct Spatial, Cell Type-Specific, and Temporal Patterns. *Immunity* 49: 560-575 e566.
470 12. Van Maele, L., D. Fougeron, D. Cayet, A. Chalon, D. Piccioli, C. Collignon, J. C. Sirard,
471 and A. M. Didierlaurent. 2019. Toll-like receptor 4 signaling in hematopoietic-lineage cells
472 contributes to the enhanced activity of the human vaccine adjuvant AS01. *Eur J Immunol*
473 49: 2134-2145.
474 13. Didierlaurent, A. M., C. Collignon, P. Bourguignon, S. Wouters, K. Fierens, M. Fochesato,
475 N. Dendouga, C. Langlet, B. Malissen, B. N. Lambrecht, N. Garcon, M. Van Mechelen,
476 and S. Morel. 2014. Enhancement of Adaptive Immunity by the Human Vaccine Adjuvant
477 AS01 Depends on Activated Dendritic Cells. *J Immunol* 193: 1920-1930.
478 14. Didierlaurent, A. M., S. Morel, L. Lockman, S. L. Giannini, M. Bisteau, H. Carlsen, A.
479 Kielland, O. Vosters, N. Vanderheyde, F. Schiavetti, D. Larocque, M. Van Mechelen, and
480 N. Garçon. 2009. AS04, an aluminum salt- and TLR4 agonist-based adjuvant system,

481 induces a transient localized innate immune response leading to enhanced adaptive
482 immunity. *J Immunol* 183: 6186-6197.
483 15. Vijayan, A., M. Rumbo, C. Carnoy, and J. C. Sirard. 2018. Compartmentalized
484 Antimicrobial Defenses in Response to Flagellin. *Trends Microbiol* 26: 423-435.
485 16. Fougeron, D., L. Van Maele, P. Songhet, D. Cayet, D. Hot, N. Van Rooijen, H. J.
486 Mollenkopf, W. D. Hardt, A. G. Benecke, and J. C. Sirard. 2015. Indirect Toll-like receptor
487 5-mediated activation of conventional dendritic cells promotes the mucosal adjuvant
488 activity of flagellin in the respiratory tract. *Vaccine* 33: 3331-3341.
489 17. Sierro, F., B. Dubois, A. Coste, D. Kaiserlian, J. P. Kraehenbuhl, and J. C. Sirard. 2001.
490 Flagellin stimulation of intestinal epithelial cells triggers CCL20-mediated migration of
491 dendritic cells. *Proc Natl Acad Sci U S A* 98: 13722-13727.
492 18. Means, T. K., F. Hayashi, K. D. Smith, A. Aderem, and A. D. Luster. 2003. The Toll-like
493 receptor 5 stimulus bacterial flagellin induces maturation and chemokine production in
494 human dendritic cells. *J Immunol* 170: 5165-5175.
495 19. Didierlaurent, A., I. Ferrero, L. A. Otten, B. Dubois, M. Reinhardt, H. Carlsen, R.
496 Blomhoff, S. Akira, J. P. Kraehenbuhl, and J. C. Sirard. 2004. Flagellin promotes myeloid
497 differentiation factor 88-dependent development of Th2-type response. *J Immunol* 172:
498 6922-6930.
499 20. Uematsu, S., K. Fujimoto, M. H. Jang, B. G. Yang, Y. J. Jung, M. Nishiyama, S. Sato, T.
500 Tsujimura, M. Yamamoto, Y. Yokota, H. Kiyono, M. Miyasaka, K. J. Ishii, and S. Akira.
501 2008. Regulation of humoral and cellular gut immunity by lamina propria dendritic cells
502 expressing Toll-like receptor 5. *Nat Immunol* 9: 769-776.
503 21. Flores-Langarica, A., K. Muller Luda, E. K. Persson, C. N. Cook, S. Bobat, J. L. Marshall,
504 M. W. Dahlgren, K. Hagerbrand, K. M. Toellner, M. D. Goodall, D. R. Withers, I. R.
505 Henderson, B. Johansson Lindbom, A. F. Cunningham, and W. W. Agace. 2018.
506 CD103(+)CD11b(+) mucosal classical dendritic cells initiate long-term switched antibody
507 responses to flagellin. *Mucosal Immunol* 11: 681-692.
508 22. Flores-Langarica, A., C. Cook, K. Muller Luda, E. K. Persson, J. L. Marshall, N. Beristain-
509 Covarrubias, J. C. Yam-Puc, M. Dahlgren, J. J. Persson, S. Uematsu, S. Akira, I. R.
510 Henderson, B. J. Lindbom, W. Agace, and A. F. Cunningham. 2018. Intestinal
511 CD103(+)CD11b(+) cDC2 Conventional Dendritic Cells Are Required for Primary
512 CD4(+) T and B Cell Responses to Soluble Flagellin. *Front Immunol* 9: 2409.
513 23. Kinnebrew, M. A., C. G. Buffie, G. E. Diehl, L. A. Zenewicz, I. Leiner, T. M. Hohl, R. A.
514 Flavell, D. R. Littman, and E. G. Pamer. 2012. Interleukin 23 production by intestinal
515 CD103(+)CD11b(+) dendritic cells in response to bacterial flagellin enhances mucosal
516 innate immune defense. *Immunity* 36: 276-287.
517 24. Anas, A. A., M. H. van Lieshout, T. A. Claushuis, A. F. de Vos, S. Florquin, O. J. de Boer,
518 B. Hou, C. Van't Veer, and T. van der Poll. 2016. Lung epithelial MyD88 drives early
519 pulmonary clearance of Pseudomonas aeruginosa by a flagellin dependent mechanism.
520 *American journal of physiology. Lung cellular and molecular physiology* 311: L219-228.
521 25. Janot, L., J. C. Sirard, T. Secher, N. Noulin, L. Fick, S. Akira, S. Uematsu, A. Didierlaurent,
522 T. Hussell, B. Ryffel, and F. Erard. 2009. Radioresistant cells expressing TLR5 control the
523 respiratory epithelium's innate immune responses to flagellin. *Eur J Immunol* 39: 1587-
524 1596.
525 26. Van Maele, L., D. Fougeron, L. Janot, A. Didierlaurent, D. Cayet, J. Tabareau, M. Rumbo,
526 S. Corvo-Chamaillard, S. Boulenouar, S. Jeffs, L. Vande Walle, M. Lamkanfi, Y. Lemoine,

527 F. Erard, D. Hot, T. Hussell, B. Ryffel, A. G. Benecke, and J. C. Sirard. 2014. Airway
528 structural cells regulate TLR5-mediated mucosal adjuvant activity. *Mucosal Immunol* 7:
529 489-500.
530 27. Lee, L. M., M. Ji, M. Sinha, M. B. Dong, X. Ren, Y. Wang, C. A. Lowell, S. Ghosh, R. M.
531 Locksley, and A. L. DeFranco. 2016. Determinants of Divergent Adaptive Immune
532 Responses after Airway Sensitization with Ligands of Toll-Like Receptor 5 or Toll-Like
533 Receptor 9. *PLoS One* 11: e0167693.
534 28. Wilson, R. H., S. Maruoka, G. S. Whitehead, J. F. Foley, G. P. Flake, M. L. Sever, D. C.
535 Zeldin, M. Kraft, S. Garantziotis, H. Nakano, and D. N. Cook. 2012. The Toll-like receptor
536 5 ligand flagellin promotes asthma by priming allergic responses to indoor allergens. *Nat*
537 *Med* 18: 1705-1710.
538 29. Munoz, N., L. Van Maele, J. M. Marques, A. Rial, J. C. Sirard, and J. A. Chabalgoity.
539 2010. Mucosal administration of flagellin protects mice from Streptococcus pneumoniae
540 lung infection. *Infect Immun* 78: 4226-4233.
541 30. Yu, F. S., M. D. Cornicelli, M. A. Kovach, M. W. Newstead, X. Zeng, A. Kumar, N. Gao,
542 S. G. Yoon, R. L. Gallo, and T. J. Standiford. 2010. Flagellin stimulates protective lung
543 mucosal immunity: role of cathelicidin-related antimicrobial peptide. *J Immunol* 185:
544 1142-1149.
545 31. Sharma, P., O. Levy, and D. J. Dowling. 2020. The TLR5 Agonist Flagellin Shapes
546 Phenotypical and Functional Activation of Lung Mucosal Antigen Presenting Cells in
547 Neonatal Mice. *Front Immunol* 11: 171.
548 32. Nempont, C., D. Cayet, M. Rumbo, C. Bompard, V. Villeret, and J. C. Sirard. 2008.
549 Deletion of flagellin's hypervariable region abrogates antibody-mediated neutralization and
550 systemic activation of TLR5-dependent immunity. *J Immunol* 181: 2036-2043.
551 33. Porte, R., D. Fougeron, N. Munoz-Wolf, J. Tabareau, A. F. Georgel, F. Wallet, C. Paget,
552 F. Trottein, J. A. Chabalgoity, C. Carnoy, and J. C. Sirard. 2015. A Toll-Like Receptor 5
553 Agonist Improves the Efficacy of Antibiotics in Treatment of Primary and Influenza Virus-
554 Associated Pneumococcal Mouse Infections. *Antimicrob Agents Chemother* 59: 6064-
555 6072.
556 34. You, Y., E. J. Richer, T. Huang, and S. L. Brody. 2002. Growth and differentiation of
557 mouse tracheal epithelial cells: selection of a proliferative population. *American journal of*
558 *physiology. Lung cellular and molecular physiology* 283: L1315-1321.
559 35. Crotta, S., S. Davidson, T. Mahlakoiv, C. J. Desmet, M. R. Buckwalter, M. L. Albert, P.
560 Staeheli, and A. Wack. 2013. Type I and type III interferons drive redundant amplification
561 loops to induce a transcriptional signature in influenza-infected airway epithelia. *PLoS*
562 *Pathog* 9: e1003773.
563 36. Naik, S. H., A. I. Proietto, N. S. Wilson, A. Dakic, P. Schnorrer, M. Fuchsberger, M. H.
564 Lahoud, M. O'Keeffe, Q. X. Shao, W. F. Chen, J. A. Villadangos, K. Shortman, and L. Wu.
565 2005. Cutting edge: generation of splenic CD8+ and CD8- dendritic cell equivalents in
566 Fms-like tyrosine kinase 3 ligand bone marrow cultures. *J Immunol* 174: 6592-6597.
567 37. Beshara, R., V. Sencio, D. Soulard, A. Barthelemy, J. Fontaine, T. Pinteau, L. Deruyter,
568 M. B. Ismail, C. Paget, J. C. Sirard, F. Trottein, and C. Faveeuw. 2018. Alteration of Flt3-
569 Ligand-dependent de novo generation of conventional dendritic cells during influenza
570 infection contributes to respiratory bacterial superinfection. *PLoS Pathog* 14: e1007360.
571 38. Hamilton, J. A. 2019. GM-CSF in inflammation. *J Exp Med*.

572 39. Greter, M., J. Helft, A. Chow, D. Hashimoto, A. Mortha, J. Agudo-Cantero, M. Bogunovic,
573 E. L. Gautier, J. Miller, M. Leboeuf, G. Lu, C. Aloman, B. D. Brown, J. W. Pollard, H.
574 Xiong, G. J. Randolph, J. E. Chipuk, P. S. Frenette, and M. Merad. 2012. GM-CSF controls
575 nonlymphoid tissue dendritic cell homeostasis but is dispensable for the differentiation of
576 inflammatory dendritic cells. *Immunity* 36: 1031-1046.
577 40. Tazi, A., F. Bouchonnet, M. Grandsaigne, L. Boumsell, A. J. Hance, and P. Soler. 1993.
578 Evidence that granulocyte macrophage-colony-stimulating factor regulates the distribution
579 and differentiated state of dendritic cells/Langerhans cells in human lung and lung cancers.
580 *J Clin Invest* 91: 566-576.
581 41. Cates, E. C., R. Fattouh, J. Wattie, M. D. Inman, S. Goncharova, A. J. Coyle, J. C.
582 Gutierrez-Ramos, and M. Jordana. 2004. Intranasal exposure of mice to house dust mite
583 elicits allergic airway inflammation via a GM-CSF-mediated mechanism. *J Immunol* 173:
584 6384-6392.
585 42. Zhou, Q., A. W. Ho, A. Schlitzer, Y. Tang, K. H. Wong, F. H. Wong, Y. L. Chua, V.
586 Angeli, A. Mortellaro, F. Ginhoux, and D. M. Kemeny. 2014. GM-CSF-licensed CD11b+
587 lung dendritic cells orchestrate Th2 immunity to Blomia tropicalis. *J Immunol* 193: 496-
588 509.
589 43. Cao, Y., E. Zhang, J. Yang, Y. Yang, J. Yu, Y. Xiao, W. Li, D. Zhou, Y. Li, B. Zhao, H.
590 Yan, M. Lu, M. Zhong, and H. Yan. 2017. Frontline Science: Nasal epithelial GM-CSF
591 contributes to TLR5-mediated modulation of airway dendritic cells and subsequent IgA
592 response. *J Leukoc Biol* 102: 575-587.
593 44. Sheih, A., W. C. Parks, and S. F. Ziegler. 2017. GM-CSF produced by the airway
594 epithelium is required for sensitization to cockroach allergen. *Mucosal Immunol* 10: 705-
595 715.
596 45. Willart, M. A., K. Deswarte, P. Pouliot, H. Braun, R. Beyaert, B. N. Lambrecht, and H.
597 Hammad. 2012. Interleukin-1alpha controls allergic sensitization to inhaled house dust
598 mite via the epithelial release of GM-CSF and IL-33. *J Exp Med* 209: 1505-1517.
599 46. Steimle, A., S. Menz, A. Bender, B. Ball, A. N. R. Weber, T. Hagemann, A. Lange, J. K.
600 Maerz, R. Parusel, L. Michaelis, A. Schafer, H. Yao, H. C. Low, S. Beier, M. Tesfazgi
601 Mebrhatu, K. Gronbach, S. Wagner, D. Voehringer, M. Schaller, B. Fehrenbacher, I. B.
602 Autenrieth, T. A. Oelschlaeger, and J. S. Frick. 2019. Flagellin hypervariable region
603 determines symbiotic properties of commensal Escherichia coli strains. *PLoS biology* 17:
604 e3000334.
605 47. Anandasabapathy, N., R. Feder, S. Mollah, S. W. Tse, M. P. Longhi, S. Mehandru, I.
606 Matos, C. Cheong, D. Ruane, L. Brane, A. Teixeira, J. Dobrin, O. Mizenina, C. G. Park,
607 M. Meredith, B. E. Clausen, M. C. Nussenzweig, and R. M. Steinman. 2014. Classical
608 Flt3L-dependent dendritic cells control immunity to protein vaccine. *J Exp Med*.
609 48. Krishnaswamy, J. K., U. Gowthaman, B. Zhang, J. Mattsson, L. Szeponik, D. Liu, R. Wu,
610 T. White, S. Calabro, L. Xu, M. A. Collet, M. Yurieva, S. Alsen, P. Fogelstrand, A. Walter,
611 W. R. Heath, S. N. Mueller, U. Yrlid, A. Williams, and S. C. Eisenbarth. 2017. Migratory
612 CD11b(+) conventional dendritic cells induce T follicular helper cell-dependent antibody
613 responses. *Sci Immunol* 2.
614

615

616 **FIGURE LEGENDS**

617

618 **Figure 1. Flagellin's adjuvant activity requires TLR5 signaling and CD4 T lymphocytes.**

619 **(A-B)** C57BL/6JRj mice (n=5) were immunized by intranasal instillation with OVA protein

620 (10 µg) alone or admixed with either $FliC_{\Delta 174-400}$ or $FliC_{TLR5mut}$ flagellin (2 µg) in PBS as a prime-

621 boost regimen administered on days 0 and 21. Serum and MdLNs were sampled on day 28 and

622 assayed respectively for OVA-specific antibodies (A) and the T cell response (B-C). **(A)** The

623 OVA-specific antibody response in the serum of immunized animals. Titers of OVA-specific IgG

624 were determined using an ELISA. **(B)** Antigen-specific lymphocyte proliferation. Cells isolated

625 from the MdLNs of immunized animals were stained with CTV and stimulated with OVA protein

626 *ex vivo* for 4 days. Representative flow cytometry plots of OVA-stimulated proliferating CD4 and

627 CD8 lymphocytes (gated on live $CD45^{+}CD3^{+}$) are shown as an index of the dilution of CTV

628 fluorescence. Proliferation is quantified as a percentage of total CD4 or CD8 cells. **(C)**

629 C57BL/6JRj mice (n=5) received an intraperitoneal injection of either 200 µg of CD4-depleting

630 antibody or an isotype control 24 hours prior to immunization with an admixture of $FliC_{\Delta 174-400}$ and

631 OVA in a prime-boost immunization regimen, as described in A-C. The titer of OVA-specific

632 antibodies in the serum of vaccinated mice was measured on day 28, as described in B. A Kruskal-

633 Wallis test with Dunn's post-test for multiple comparisons was used to assess statistical

634 significance. The results were expressed as the mean ± SD and were representative of two

635 experiments.

636

637 **Figure 2. TLR5 engagement on AECs promotes GM-CSF production.**

638 Airway epithelial cells from mice were grown at air liquid interface and stimulated by $FliC_{\Delta 174-400}$
639 (10 µl of 1 µg/ml of $FliC_{\Delta 174-400}$ were added to the air-exposed apical side). At the indicated
640 times, AECs were sampled to prepare mRNA and cDNA for RT-qPCR and basolateral
641 supernatants were sampled for cytokine analysis using an ELISA. The dotted line indicates the
642 detection limit of the assay. (**A-B**) The flagellin-mediated activation of AECs from C57BL/6JRj
643 (WT, n=9-10) was analyzed. **(A)** The time course of flagellin-mediated gene transcription. The
644 AECs were lysed to extract RNA and gene expression was quantified as described in the Materials
645 and Methods section. **(B)** Secretion of GMCSF at 24h post-treatment, measured using an ELISA
646 according to the manufacturer's instruction. Intergroup comparisons were performed using a
647 Mann-Whitney unpaired t test. **(C)** The TLR5-dependent stimulation. Levels of GM-CSF in the
648 supernatant of $FliC_{\Delta 174-400}$-stimulated AECs derived from *Tlr5*$^{-/-}$ or WT mice (n=6) were measured
649 at the indicated times using an ELISA. **(D)** C57BL/6JRj mice (n=8 per group) were treated (or not)
650 intranasally with $FliC_{\Delta 174-400}$ (2 µg) in PBS. Bronchoalveolar lavages were sampled at 4 h and 8 h,
651 and GM-CSF levels were measured using an ELISA. Time points were compared using a Kruskal-
652 Wallis one-way ANOVA with Dunn's post-test. The results were representative of three
653 experiments.
654
655 **Figure 3. The *in vitro* activation of FLT3L-derived BMDCs by flagellin-stimulated AECs**
656 **depends on GM-CSF.**
657 **(A)** Schematic representation of the experimental design. FLT3L-derived BMDCs from *Tlr5*$^{-/-}$
658 mice were stimulated for 18 h with conditioned medium from $FliC_{\Delta 174-400}$-treated AECs in the
659 presence of GM-CSF-neutralizing antibodies or an isotype antibody control. **(B)** Representative
660 flow cytometry plots of stimulated, FLT3L-derived BMDCs gated on the cDC2 (live

661 $CD45^{+}CD11c^{+}MHCII^{+}CD11b^{+}CD24^{dim}$) population expressing the activation markers CD80 and
662 CD86. Untreated BMDCs were used to estimate the background fluorescence intensity. **(C)**. Total
663 numbers of activated cDC2 cells and the median fluorescence intensity for CD80 and CD86 on
664 cDC2s after treatment. Groups were compared using a two-way ANOVA with Tukey's post-test.
665 The results were representative of four experiments.
666
667 **Figure 4. GM-CSF from AECs licenses DCs to stimulate antigen-specific CD4 lymphocytes.**
668 **(A)** Schematic representation of the experimental design. FLT3L-derived BMDCs from *Tlr5*$^{-/-}$
669 mice were stimulated for 18 h with conditioned medium from $FliC_{\Delta 174-400}$-treated AECs in the
670 presence of GM-CSF-neutralizing antibodies or an isotype antibody control. The BMDCs were
671 next washed and incubated for 4 h with $OVA_{323-339}$ MHCII-specific peptide before co-culture for
672 4 days with CTV-stained, naïve, OVA-specific CD4 lymphocytes from OTII mice. **(B-C)**
673 Proliferation of CD4 T cells (gated as live $CD45^{+}CD3^{+}CD4^{+}V\alpha2^{+}$). The percentage of dividing
674 CD4 T cells (as measured by the dilution of CTV fluorescence) was measured using flow
675 cytometry. Mock BMDCs (not conditioned) co-cultured with CTV-stained CD4 T cells were used
676 to estimate background levels **(B)**. Representative histograms of CTV dilution. **(C)** Quantification
677 of $CD4^{+}$ T cell proliferation, using independent conditioned medium (n=5). Groups were
678 compared in a two-way ANOVA with Tukey's post-test. The results were representative of three
679 experiments.
680
681 **Figure 5. GM-CSF regulates the flagellin-mediated activation of DCs in MdLNs.**
682 **(A)** Experimental design. C57BL/6JRj mice (n=5 to 6) were treated with a GM-CSF-neutralizing
683 antibody or an isotype antibody control 2 hours prior to and then upon administration of flagellin

684 $FliC_{\Delta 174-400}$. All treatments were given intranasally in a total of volume of 30 µl per treatment. The
685 DC populations in the MdLN were analyzed at 18 hours, using flow cytometry. Dendritic cells
686 were identified as $CD11c^{+}MHCII^{+}$ cells within the live $CD45^{+}Lin^{neg}$ population. **(B)**
687 Representative dot plots of MdLN cDCs. **(C)** The numbers of cDC2s are quoted as the percentage
688 of total $CD45^{+}$ cells. **(D)** Activation of MdLN cDC2s. The numbers of cDC2s expressing
689 CD80 and CD86 are quoted as a percentage of total $CD45^{+}$ cells. **(E)** Median fluorescence intensity
690 of CD80 in the activated cDC2 population. Groups were compared using a Kruskal-Wallis one-
691 way ANOVA with Dunn's post-test. The results were representative of three experiments.
692
693 **Figure 6. Neutralization of GM-CSF reduces flagellin's adjuvant activity.**
694 **(A)** Experimental design. C57BL/6JRj mice (n=8) were immunized by intranasal instillation with
695 OVA protein (10 µg) alone or with OVA and flagellin $FliC_{\Delta 174-400}$ (2 µg) in PBS as a prime-boost
696 regimen administered on days 0 and 21. Two hours prior to and upon immunization, the animals
697 were treated intranasally with GM-CSF-neutralizing antibodies or an isotype antibody control
698 (60 µg) in PBS. Serum, BAL, and MdLNs were sampled on day 28 to measure the OVA-specific
699 T cell response (B) and OVA-specific antibody titer (C), respectively. **(B)** Antigen-specific
700 lymphocyte proliferation. Cells isolated from the MdLNs of immunized animals were stained with
701 CTV and stimulated with OVA protein *ex vivo* for 4 days. Representative flow cytometry plots of
702 OVA-stimulated proliferating live $CD45^{+}CD3^{+}CD4^{+}$ are shown as a measure of the CTV
703 fluorescence dilution. Proliferation was quantified as a percentage of total $CD4^{+}$ T cells. **(C)** The
704 OVA-specific antibody response in serum and BAL of immunized animals. The dotted line
705 indicates the OVA-specific IgG titers elicited in OVA/PBS immunized animals. Levels of OVA-

706 specific IgG were measured using an ELISA. Groups were compared using a Mann-Whitney
707 unpaired t test.
708

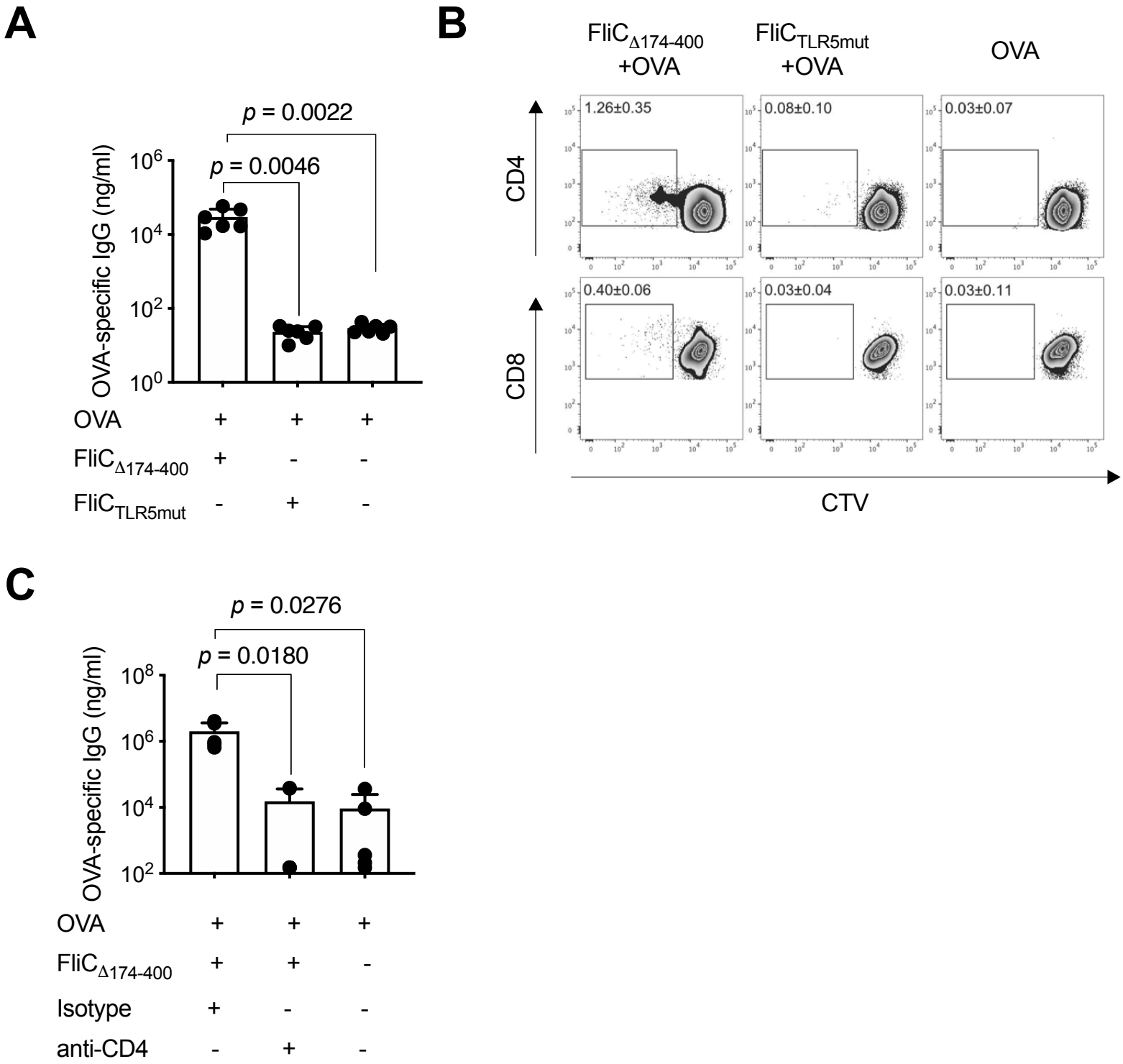
A
p = 0.0022
p = 0.0046
OVA-specific IgG (ng/ml)
10^6
10^4
10^2
10^0
OVA + + +
FliC Δ174-400 + - -
FliC TLR5mut - + -
B
FliC Δ174-400 +OVA
FliC TLR5mut +OVA
OVA
CD4
CD8
1.26±0.35
0.08±0.10
0.03±0.07
0.40±0.06
0.03±0.04
0.03±0.11
CTV
C
p = 0.0276
p = 0.0180
OVA-specific IgG (ng/ml)
10^8
10^6
10^4
10^2
OVA + + +
FliC Δ174-400 + + -
Isotype + - -
anti-CD4 - + -

Figure 1

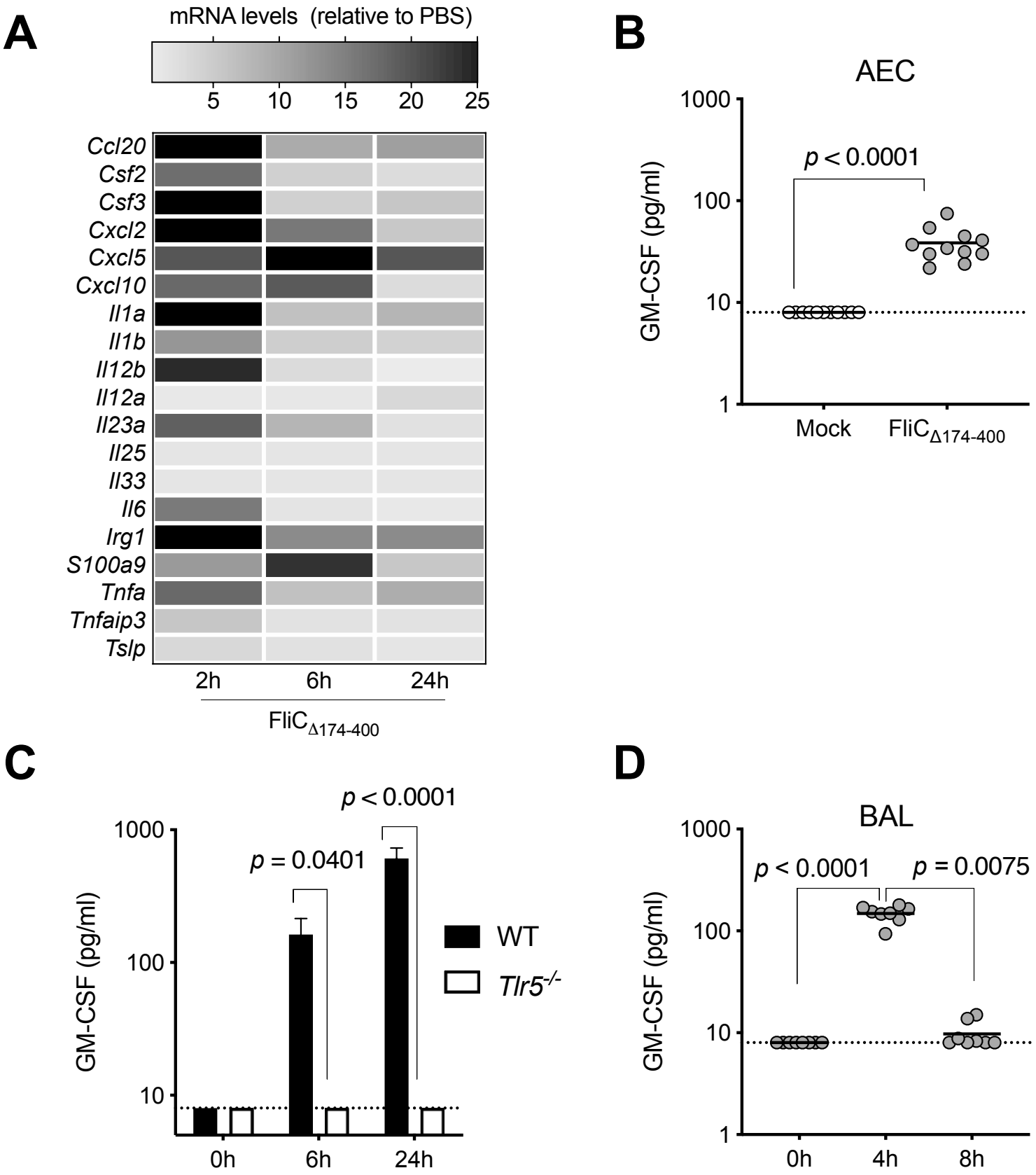
A
mRNA levels (relative to PBS)
5
10
15
20
25
Ccl20
Csf2
Csf3
Cxcl2
Cxcl5
Cxcl10
Il1a
Il1b
Il12b
Il12a
Il23a
Il25
Il33
Il6
Irg1
S100a9
Tnfa
Tnfaip3
Tslp
2h
6h
24h
FliC$_{\Delta 174-400}$
B
AEC
GM-CSF (pg/ml)
1000
100
10
1
p < 0.0001
Mock
FliC$_{\Delta 174-400}$
C
GM-CSF (pg/ml)
1000
100
10
p = 0.0401
p < 0.0001
WT
Tlr5$^{-/-}$
0h
6h
24h
D
BAL
GM-CSF (pg/ml)
1000
100
10
1
p < 0.0001
p = 0.0075
0h
4h
8h

Figure 2

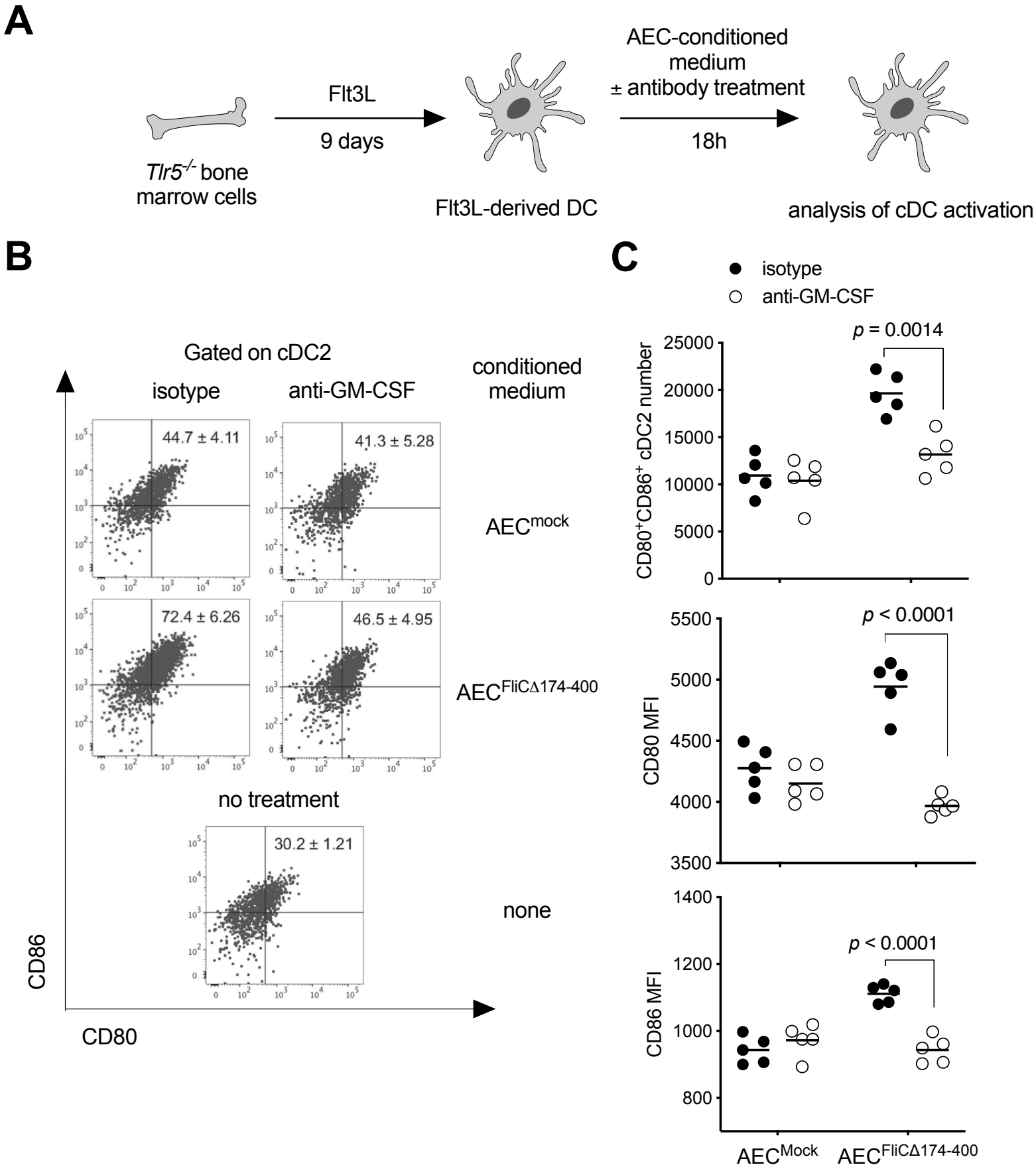
A
Flt3L
9 days
Tlr5-/- bone marrow cells
Flt3L-derived DC
AEC-conditioned medium
± antibody treatment
18h
analysis of cDC activation
B
Gated on cDC2
isotype
anti-GM-CSF
conditioned medium
44.7 ± 4.11
41.3 ± 5.28
AECmock
72.4 ± 6.26
46.5 ± 4.95
AECFliCΔ174-400
no treatment
30.2 ± 1.21
none
CD86
CD80
C
isotype
anti-GM-CSF
p = 0.0014
CD80+CD86+ cDC2 number
p < 0.0001
CD80 MFI
p < 0.0001
CD86 MFI
AECMock
AECFliCΔ174-400

Figure 3

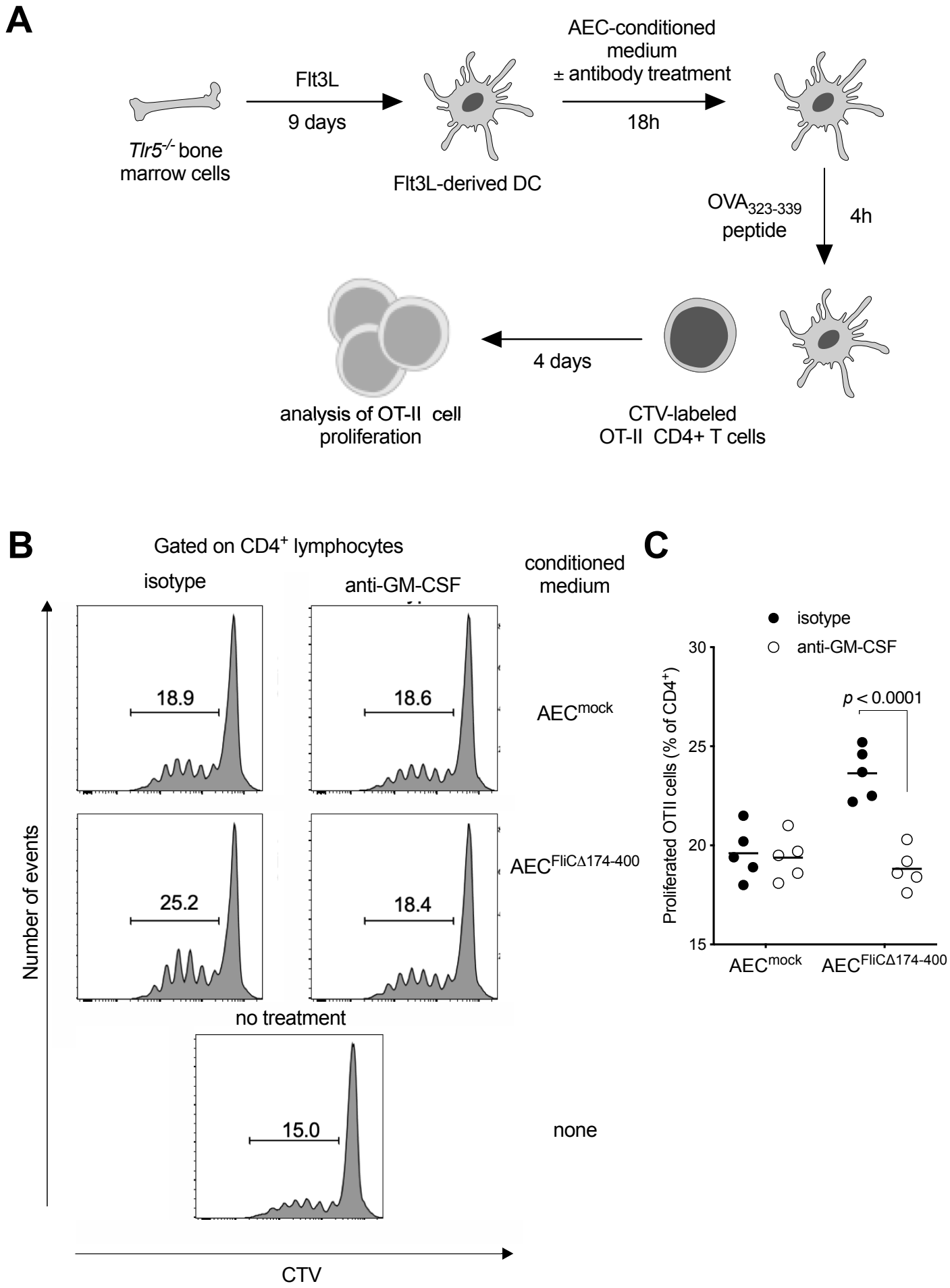
A
Flt3L
9 days
Tlr5-/- bone marrow cells
Flt3L-derived DC
AEC-conditioned medium
± antibody treatment
18h
OVA323-339 peptide
4h
4 days
analysis of OT-II cell proliferation
CTV-labeled OT-II CD4+ T cells
B
Gated on CD4+ lymphocytes
isotype
anti-GM-CSF
conditioned medium
18.9
18.6
AECmock
25.2
18.4
AECFliCΔ174-400
no treatment
15.0
none
Number of events
CTV
C
isotype
anti-GM-CSF
p < 0.0001
Proliferated OTII cells (% of CD4+)
30
25
20
15
AECmock
AECFliCΔ174-400

Figure 4

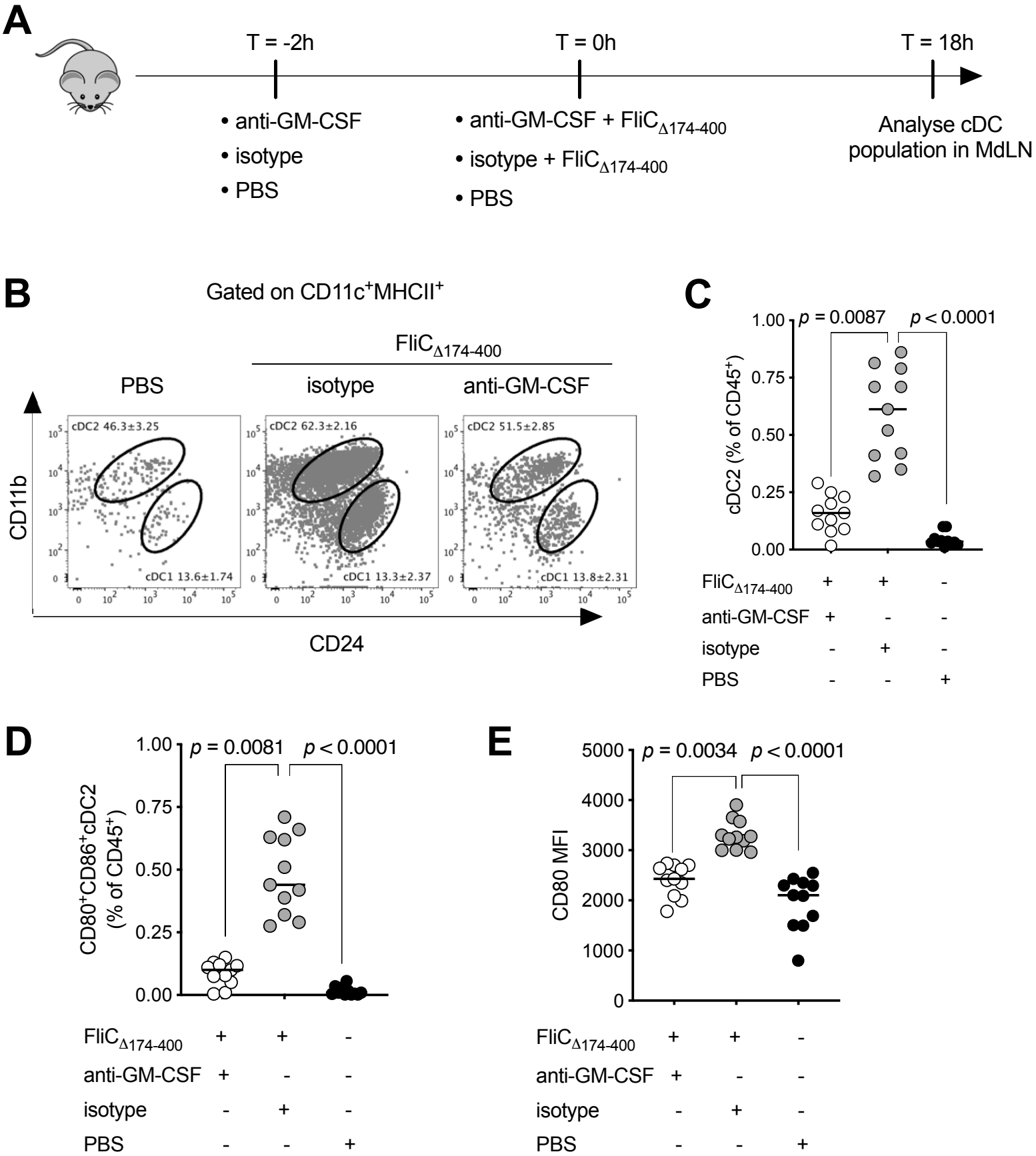
A
T = -2h
T = 0h
T = 18h
• anti-GM-CSF
• isotype
• PBS
• anti-GM-CSF + FliC$_{\Delta174-400}$
• isotype + FliC$_{\Delta174-400}$
• PBS
Analyse cDC population in MdLN
B
Gated on CD11c$^+$MHCII$^+$
FliC$_{\Delta174-400}$
PBS
isotype
anti-GM-CSF
cDC2 46.3±3.25
cDC1 13.6±1.74
cDC2 62.3±2.16
cDC1 13.3±2.37
cDC2 51.5±2.85
cDC1 13.8±2.31
CD11b
CD24
C
p = 0.0087
p < 0.0001
cDC2 (% of CD45$^+$)
FliC$_{\Delta174-400}$ + + -
anti-GM-CSF + - -
isotype - + -
PBS - - +
D
p = 0.0081
p < 0.0001
CD80$^+$CD86$^+$cDC2 (% of CD45$^+$)
FliC$_{\Delta174-400}$ + + -
anti-GM-CSF + - -
isotype - + -
PBS - - +
E
p = 0.0034
p < 0.0001
CD80 MFI
FliC$_{\Delta174-400}$ + + -
anti-GM-CSF + - -
isotype - + -
PBS - - +

Figure 5

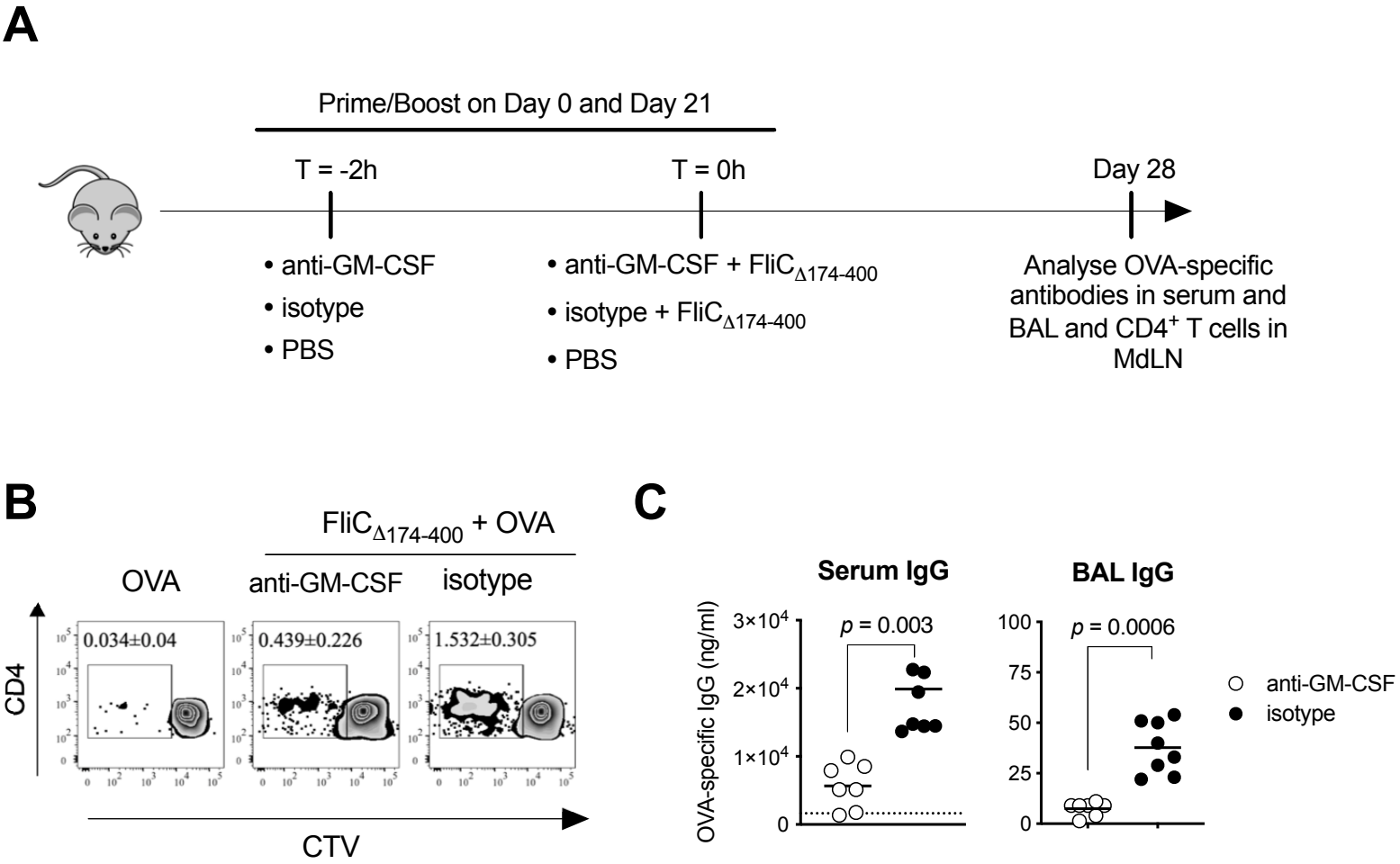
A
Prime/Boost on Day 0 and Day 21
T = -2h
T = 0h
Day 28
• anti-GM-CSF
• isotype
• PBS
• anti-GM-CSF + FliC$_{\Delta 174\text{-}400}$
• isotype + FliC$_{\Delta 174\text{-}400}$
• PBS
Analyse OVA-specific antibodies in serum and BAL and CD4^{+} T cells in MdLN
B
FliC$_{\Delta 174\text{-}400}$ + OVA
OVA
anti-GM-CSF
isotype
CD4
0.034±0.04
0.439±0.226
1.532±0.305
CTV
C
Serum IgG
BAL IgG
OVA-specific IgG (ng/ml)
3×10^{4}
2×10^{4}
1×10^{4}
0
p = 0.003
100
75
50
25
0
p = 0.0006
anti-GM-CSF
isotype

Figure 6

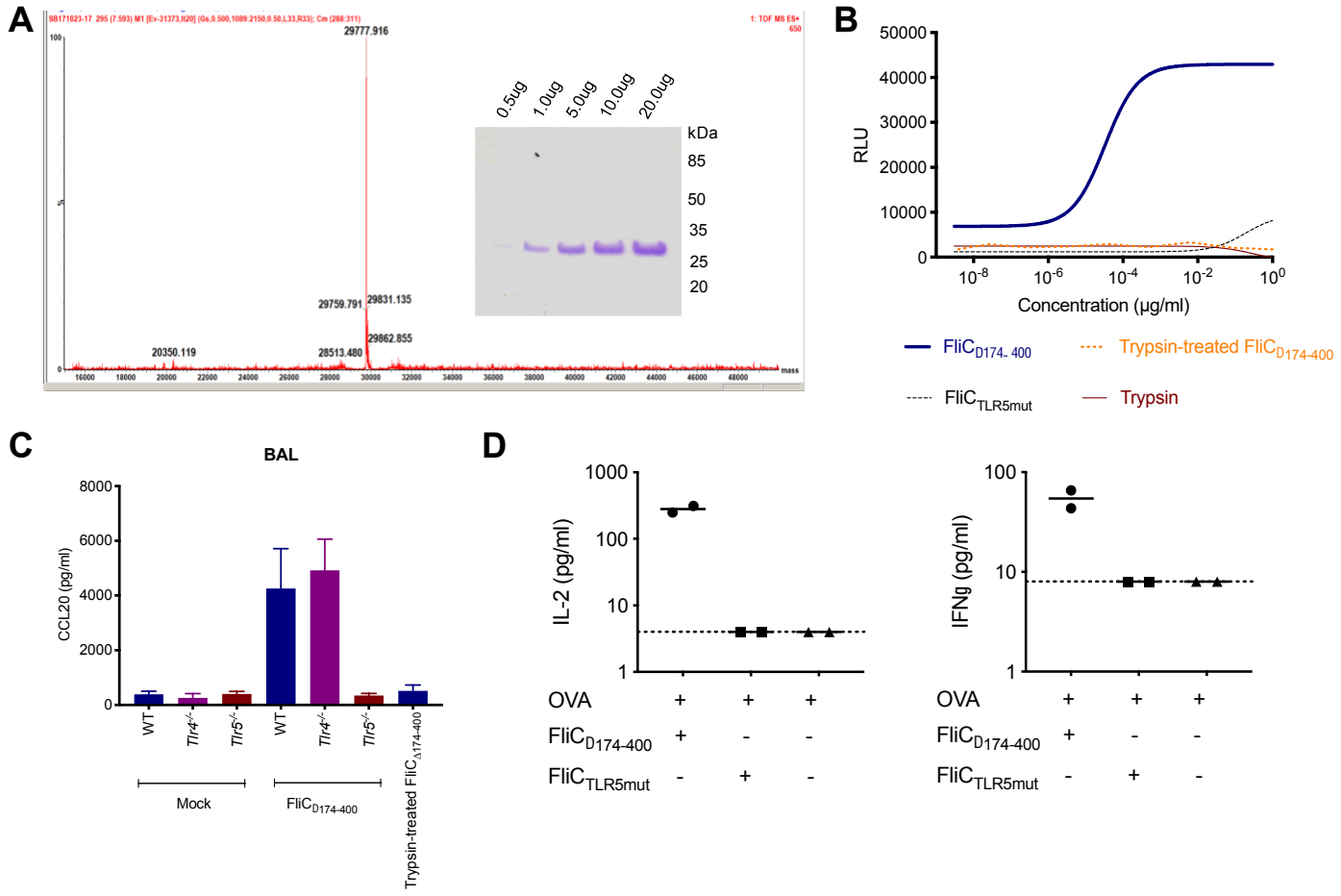

Figure S1. Flagellin stimulates OVA-specific cytokine production by mediastinal lymph node cells. The biophysical characteristics of recombinant flagellin FliC$_{\Delta 174\text{-}400}$ (expressed and purified from *E. coli)* was assessed as described in A-C. **(A)**. Mass spectrometry analysis of the protein yielded a single peak of the expected molecular weight (29 kDa). The insert shows the SDS-PAGE analysis of the indicated amounts (in µg) of recombinant protein, followed by Coomassie staining. **(B)** *In vitro* activity of the recombinant protein, as measured in a Caco-2 cell-based assay. The reporter cell line contains a luciferase transgene that is driven by the *CCL20* promoter. Flagellin FliC$_{\Delta 174\text{-}400}$ that lacked TLR5 activity (FliC$_{TLR5mut}$) and trypsin-treated FliC$_{\Delta 174\text{-}400}$ were used as controls. **(C)** *In vivo* functional analysis of FliC$_{\Delta 174\text{-}400}$. *Tlr5*$_{-/-}$, *Tlr4*$_{-/-}$ or C57Bl/6JRj (WT) mice were given an intranasal instillation of 2 µg of FliC$_{\Delta 174\text{-}400}$, PBS, or trypsin-treated FliC$_{\Delta 174\text{-}400}$. BAL samples were taken at 6 hours, and the CCL20 level was determined using an ELISA. Cellular response to vaccination was analyzed as follows in **(D)**: C57BL/6JRj mice (n=5) were immunized by intranasal instillation with OVA protein (10 µg) alone or OVA admixed with either FliC$_{\Delta 174\text{-}400}$ or FliC$_{TLR5mut}$ flagellin (2 µg) in PBS as a prime-boost regimen administered on days 0 and 21. Mediastinal lymph nodes were sampled on day 28 and pooled, and OVA-specific cytokine production was assessed. Levels of IFNγ and IL-2 levels in the supernatant of OVA-stimulated MdLN cells were measured using an ELISA. The dotted line indicates the assay's limit of detection. The results were representative of two experiments (a pool of two MdLNs and a pool of three MdLNs per group).

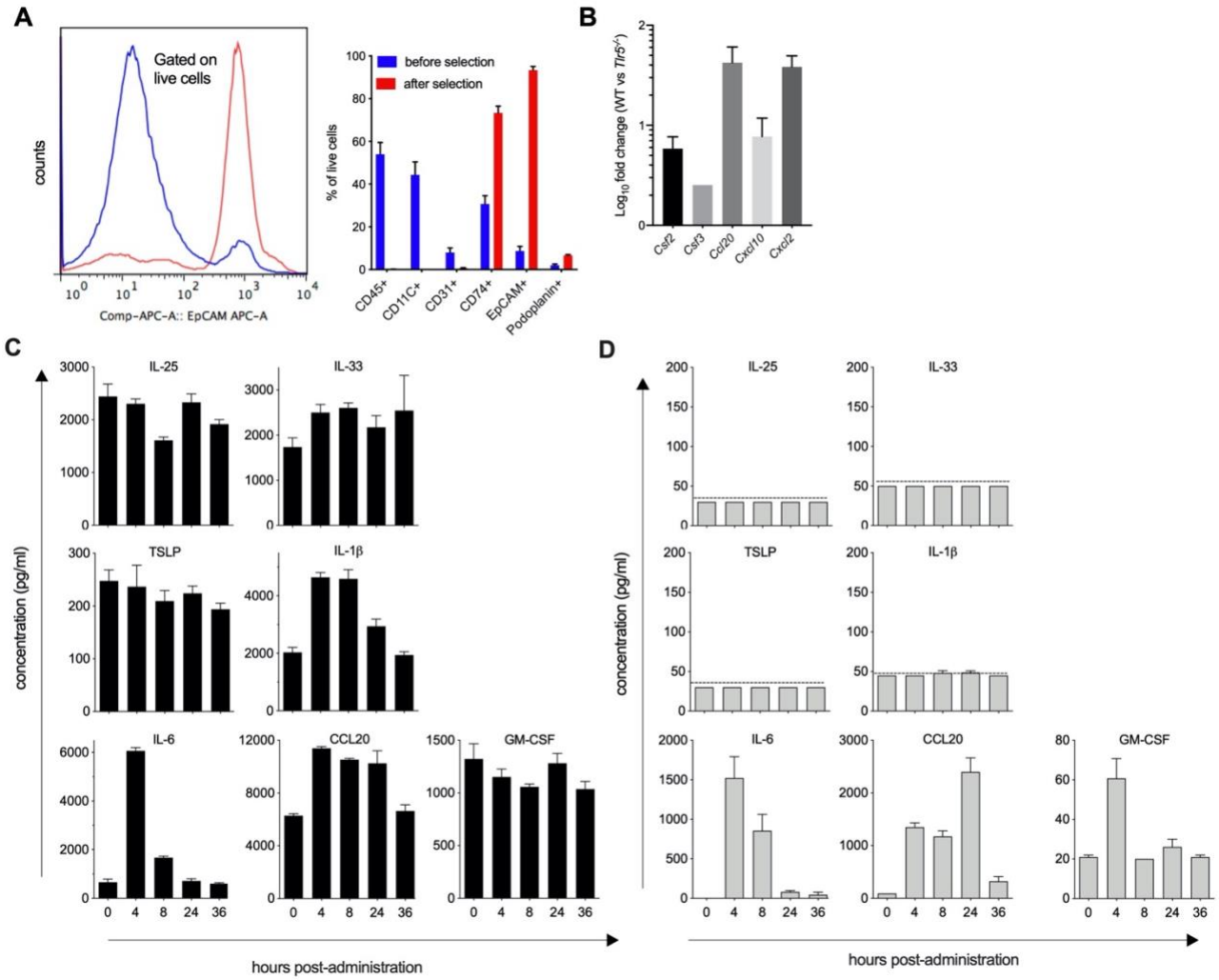

Figure S2. Airway epithelium and conducting airways respond to flagellin stimulation

(A-B) Freshly isolated lung alveolar epithelial cells are activated by flagellin. Lungs that were isolated from *Tlr5*$_{-/-}$ or C57BL/6JRj (WT) mice were digested with dispase to obtain a cell suspension. Following negative selection using magnetic beads and antibodies specific for CD45, CD31, and Ter119, the cells were analyzed for purity **(A)**. The cells before and after selection were stained with an antibody specific for airway epithelial cells (Epcam$_{+}$). To further differentiate between type I and type II alveolar epithelial cells, additional markers such as podoplanin (type I) and CD74 (type II) were included in the flow cytometry analysis **(B)**. The alveolar epithelial cells were allowed to rest for 18 hours after isolation. Next, the cells were counted and seeded at $2 \times 10_5$ in each well of a 96 well and stimulated with 1 µg/ml of FliC$_{\Delta 174\text{-}400}$ in PBS for 6 hours. The RNA was isolated from stimulated cells and analyzed for the upregulation of the indicated genes. **(C-D)** Expression of potential DC-activating cytokines in mouse lung and broncho-alveolar lavages in response to intranasal administration of native flagellin. C57BL/6JRj mice (n=4 per group) were intranasally administered with native flagellin FliC (1 µg in 20 µl PBS). Total lung and broncho-alveolar lavages were sampled at 2, 4, 8, 18, 24, and 36 hours post-instillation. Lung protein extracts **(C)** and broncho-alveolar lavages **(D)** were prepared and cytokines were then measured by specific ELISA. The dotted line indicates the detection limit of the ELISA assay Data represent the mean ± SEM and are representative of 1-2 experiments (*$p<0.05$).

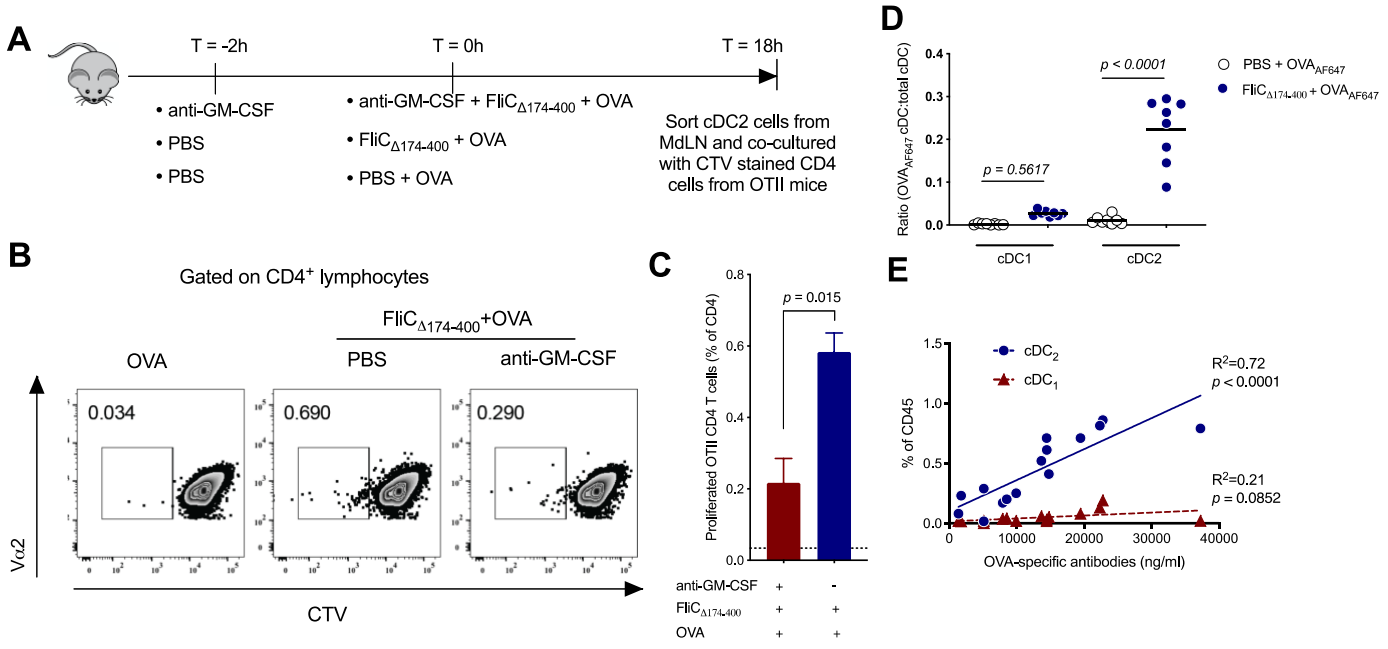

Figure S3. GM-CSF regulates the flagellin-mediated adjuvant effect by modulation of type 2 conventional dendritic cells

(A-C) GM-CSF regulates the flagellin-mediated DC-dependent priming of CD4 lymphocytes. **(A)** Experimental design. C57BL/6JRj mice (n=5) were treated with a GM-CSF-neutralizing antibody or PBS two hours prior to and then upon administration of flagellin FliC$_{\Delta174-400}$. All treatments were given intranasally in a total of volume of 30 µl per treatment (OVA protein (10 µg) alone or with OVA and flagellin FliC$_{\Delta174-400}$ (2 µg)). At 18 hours, MdLN were sampled, and cDC2 were sorted as CD11c$^+$MHCII$^+$CD11b$^+$CD103^{neg} cells within the live CD45$^+$Lin^{neg}SiglecF^{neg} population. Then cells were co-cultured for 4 days with CTV-stained, naïve, OVA-specific CD4 lymphocytes from OTII mice. **(B)** Proliferation of CD4 T cells. The percentage of dividing CD4 T cells (as measured by the dilution of CTV fluorescence into live CD45$^+$CD3$^+$CD4$^+$Vα2$^+$ cells) was measured using flow cytometry. **(C)** Representative histograms of CTV dilution. Groups were compared using a Mann-Whitney unpaired t test. **(D)** The flagellin-activated cDC2s that capture antigen following intranasal instillation are found in the MdLNs. C57BL/6JRj mice (n=8) were intranasally administered with 10 µg of OVA$_{AF647}$ or 2 µg of FliC$_{\Delta174-400}$ in PBS. The mice's MdLNs were sampled 18 hours after immunization and stained for cDC1s and cDC2s. Ratios of OVA$_{AF647}$-associated cDC1s and cDC2s to total cDCs in the MdLNs. Groups were compared in a one-way ANOVA with Tukey's post-test. The results were representative of two independent experiments. **(E).** Neutralization of GM-CSF is correlated with the adjuvant effect of flagellin. The correlation between cDC1 or cDC2 counts and the titer of OVA-specific antibodies elicited by the immunization with FliC$_{\Delta174-400}$ and OVA along with GM-CSF-neutralizing antibodies. The results from OVA-specific antibodies that were elicited in animals after a prime-boost with FliC$_{\Delta174-400}$ and GM-CSF antibody were plotted against the total frequencies of cDC2s and cDC1s (gated on CD45 live cells) in the MdLNs (18 hours) after exposure to FliC$_{\Delta174-400}$ and GM-CSF antibody. Correlations were assessed by calculating Pearson's coefficient.